

American University in Cairo

AUC Knowledge Fountain

Theses and Dissertations

Student Research

Winter 1-31-2023

Lignin Nanoparticles Comparative Study for their Emulsifying, Antibacterial and Antioxidant Properties

Matta Asaad Mesak Ebaid
matta.assad@aucegypt.edu

Follow this and additional works at: <https://fount.aucegypt.edu/etds>



Part of the [Food Science Commons](#)

Recommended Citation

APA Citation

Ebaid, M. (2023). *Lignin Nanoparticles Comparative Study for their Emulsifying, Antibacterial and Antioxidant Properties* [Master's Thesis, the American University in Cairo]. AUC Knowledge Fountain. <https://fount.aucegypt.edu/etds/1955>

MLA Citation

Ebaid, Matta Asaad Mesak. *Lignin Nanoparticles Comparative Study for their Emulsifying, Antibacterial and Antioxidant Properties*. 2023. American University in Cairo, Master's Thesis. *AUC Knowledge Fountain*. <https://fount.aucegypt.edu/etds/1955>

This Master's Thesis is brought to you for free and open access by the Student Research at AUC Knowledge Fountain. It has been accepted for inclusion in Theses and Dissertations by an authorized administrator of AUC Knowledge Fountain. For more information, please contact thesisadmin@aucegypt.edu.



The American
University in Cairo
الجامعة الأمريكية بالقاهرة
Graduate Studies

Lignin nanoparticles comparative study for their emulsifying, antibacterial and antioxidant properties

A THESIS SUBMITTED BY

Matta Asaad Mesak Ebaid

TO THE

Department of Chemistry

Date

11.08.2022

in partial fulfillment of the requirements for the degree of

Master of Science in Chemistry, with concentration in food
chemistry

Declaration of Authorship

I, Matta Asaad Mesak Ebaid, declare that this thesis titled, “Lignin nanoparticles comparative study for their emulsifying, antibacterial and antioxidant properties” and the work presented in it are my own. I confirm that:

- This work was done wholly or mainly while in candidature for a research degree at this University.
- Where any part of this thesis has previously been submitted for a degree or any other qualification at this University or any other institution, this has been clearly stated.
- Where I have consulted the published work of others, this is always clearly attributed.
- Where I have quoted from the work of others, the source is always given. With the exception of such quotations, this thesis is entirely my own work.
- I have acknowledged all main sources of help.
- Where the thesis is based on work done by myself jointly with others, I have made clear exactly what was done by others and what I have contributed myself.

Signed:

Matta Asaad

Date:

11.08.2022

Abstract

Converting lignin, the second most natural abundant polymer on earth, into lignin nanoparticles (LNPs) form has potential applications. LNPs' emulsifying, antibacterial and antioxidant properties of three different lignins, softwood kraft lignoboost (LB), hardwood birch (BB) and alkali protobind 1000 (PB) were evaluated in a comparative study at different pH and concentrations. Lower ionic strength of 5 millimole (mM) citric acid (CA) and pH of 7 were found to be the most optimum conditions for emulsion formation. Comparison among the two homogenization techniques revealed that microfluidizer is favored in case of BB- and PB-LNPs based emulsions, while ultrasonication is optimum in case of LB-LNPs based emulsions. LNPs' concentrations were found directly in proportion with their emulsifying activity to stabilize emulsions. LNPs based rapeseed oil (RO)/water emulsions showed slightly better yield than LNPs based hexadecane (HD)/water emulsions in terms of particle size distribution (PSD) in PB-LNPs and LB-LNPs based samples while the opposite in case BB-LNPs emulsions. As an emulsifier, PB-LNPs showed the highest effect versus LP- LNPs least effective. In terms of antioxidant activity, BB-LNPs showed the highest effect represented by 83 % of 2,2-diphenyl-1-picrylhydrazyl (DPPH) inhibition while LB-LNPs' DPPH inhibition was the lowest by 67 at 0.5 w/w% LNPs concentration. Microbiologically, LNPs exhibited strong inhibition against gram positive *Staphylococcus aureus* by achieving 3 logs of reduction; however, found less effective against gram negative *Escherichia coli* (*E. coli*) without major reduction. This study expands on the potential applications of LNPs to be employed in food, agriculture, and pharmaceutical industries.

Keywords: antioxidant; antibacterial; emulsifiers; emulsions; homogenization; lignin nanoparticles (LNPs); microfluidization; ultrasonication.

Acknowledgements

I thank the American University in Cairo in supporting me during this work establishing collaborative research study mediated by Prof. Dr. Mohamed Farag. I thank Helsinki University in Finland for their supervision represented by Prof. Dr. Kirsi S. Mikkonen (Associate professor, Academy Research Fellow, Department of Food and Nutrition) and Dr. Patricia Figueiredo (Postdoctoral Researcher, Department of Food and Nutrition) who had the initiative proposal, conduct the experimental work using the laboratory facility. and edited my thesis. Extending my appreciation to Prof. Dr. Per Saris (professor, Department of Microbiology) for supporting me for the microbiological testing and utilizing his lab and resources. Thanks for Dr.-Ing. Ahmed Zayed (Postdoc. at the Institute of Bioprocess Engineering, Technical University of Kaiserslautern, Germany) for his support regarding the Analysis of Variance (ANOVA) statistical analysis. Thanks for the defense committee for their comments and discussion of this thesis work represented by Dr. Nermeen ElKasabgy (External Examiner) Associate Professor, Faculty of Pharmacy, Cairo University Dr. Mayyada El-Sayed (Internal Examiner) Associate Professor, Department of Chemistry, SSE, AUC Dr. Mohamed Salama (Moderator) Associate Professor, Institute of Global Health and Human Ecology, SSE, AUC. I am also deeply thankful for my main supervisor Prof. Dr. Mohamed A. Farag (Professor Cairo University & visiting Professor American University in Cairo) or all his continuous support during this work from the start till its final editing and correcting my written thesis.

Contents

Declaration of Authorship	2
Abstract.....	3
Acknowledgements.....	4
Contents.....	5
List of figures	7
List of tables.....	10
List of abbreviations.....	12
List of symbols	13
Chapter 1: Introduction.....	14
1.1 Lignin background.....	14
1.2 Lignin isolation and depolymerization from biomass and types	15
1.3 Lignin functional properties.....	16
1.3.1 Emulsification	18
1.3.2 Antibacterial	19
1.3.3 Antioxidant activity	20
Chapter 2: Experimental section	20
1.1 Materials and methods.....	21
1.2 Preparation of LNPs	21
1.3 LNPs as an emulsion stabilizer	22
1.3.1 Preparation of oil-in-water emulsions using microfluidizer	22
1.3.2 Preparation of oil-in-water emulsions using ultrasonication	23
1.3.3 Emulsion characterization.....	23
1.3.3.1 Optical Microscopy	24
1.3.3.2 PSD characterization	24
1.3.3.3 Emulsion stability kinetics	25
1.4 Antibacterial effects of LNPs	25
1.5 Total phenolic content of LNPs-based emulsions	27
1.6 Antioxidant activity of LNPs.....	27
Chapter 3: Results and discussion	28

1.1	LNPs as an emulsion stabilizer	28
1.1.1	Optimization of LNPs in different ionic strengths and pH.....	28
1.1.2	Preparation of oil-in-water emulsions using microfluidizer	31
1.1.3	Preparation of emulsions using ultrasonication utilizing RO and HD ...	36
1.2	Phenolic content determination of LNPs-based emulsions	42
1.3	Antioxidant activity of LNPs.....	44
1.4	Antibacterial inhibition of LNPs	46
Chapter 4: Conclusions and future directions.....		51
Chapter 5: References.....		52

List of figures

Figure 1.1 The main three cinnamoyl alcohol monomers present in lignin.	14
Figure 1.2 β -O-4 bond typical connection type in lignin's monomers highlighted in the black cycle.	15
Figure 1.3 Figure shows simple representation of how emulsification of two immiscible liquids (water and oil) with the aid of the LNPs (emulsifying agent) occurs.	18
Figure 2.1 Diagrammatic flow of the major steps performed in this study including: LNPs preparation and testing their different functions of emulsifying, antibacterial, antioxidant properties and phenolic content.	21
Figure 2.2 Diagrammatic sketch showing the steps of preparing emulsion, homogenization and its characterization.	22
Figure 2.3 Diagrammatic flow chart showing steps of preparing, homogenizing, and characterizing 5% of RO and HD emulsions homogenized using ultrasonication by physical and microscopical examination, droplet size and stability.	23
Figure 2.4 Diagram showing the general outline to screen bacterial inhibition of 0.5 w/w% of LB-, BB- and PB-LNPs around against <i>E. coli</i> , and <i>Staphylococcus aureus</i> strains. Each colored three cycles indicate the three replicates of different level of dilution to be screened.	26
Figure 2.5 A diagrammatic sketch simplifies the steps to screen and identify number of bacterial logs of inhibition generated by BB LNPs against <i>Staphylococcus aureus</i> strain. The plates were plated using surface spread technique in triplicates after incubation.	27
Figure 3.1 Representative pictures of the physical appearance and optical microscopy (40x magnifications) of 0.1 w/w% BB-LNPs-based emulsions, containing 5% RO, prepared in 5 and 10 mM CA buffer at pH 5, 6 and 7 using microfluidizer, at the day of preparation.	29
Figure 3.2 PSD graphs for 0.1 w/w% BB-LNPs-based 5% RO emulsions, at different ionic strengths and pH at day 0, 1 and 7.	30
Figure 3.3 TSI values indicating the stability of 0.1 w/w% BB-LNPs-based 5% RO emulsions prepared with different ionic strengths (5 and 10 mM CA buffers) and pH 5, 6 and 7, at different height levels (global, bottom, and top) over 14 days.	30
Figure 3.4. PSD plots of 0.1, 0.25 and 0.5 w/w% BB-LNPs-based emulsions, containing 5% RO, prepared in 5 mM CA buffer at pH 6 and 7 using microfluidizer, at day 0, 1, 7, 14, and 30.	32

Figure 3.5 Representative pictures of the physical appearance and optical microscopy (40x and 100x magnifications) of 0.1, 0.25 and 0.5 w/w% BB-LNPs-based emulsions, containing 5% RO, prepared in 5 mM CA buffer at pH 6 and 7 using microfluidizer, at the day of preparation.32

Figure 3.6 Global, bottom, and top TSI stability values for 0.1, 0.25 and 0.5 w/w% BB-LNPs-based emulsions, containing 5% RO, prepared in 5 mM CA buffer at pH 6 and 7 using microfluidizer, over one month.....33

Figure 3.7 PSD plots of 0.1, 0.25 and 0.5 w/w% PB LNPs forming 5% RO emulsions at pH 6 and 7 using microfluidizer at 0, 1-, 7-, 14-, and 30-days intervals.34

Figure 3.8 Representative pictures of the physical appearance and optical microscopy (100x magnifications) of 0.1, 0.25 and 0.5 w/w% PB-LNPs-based emulsions, containing 5% RO, prepared in 5 mM CA buffer at pH 6 and 7 using microfluidizer, at the day of preparation.34

Figure 3.9 Global, bottom, and top TSI stability indicators for various formed 5% RO emulsions using 0.1, 0.25 and 0.5 w/w% BB LNPs at pH6 and 7 over a month duration interval.35

Figure 3.10 Representative pictures of the physical appearance of LB-LNPs-based emulsions, containing 5% RO, prepared in 5 mM CA buffer at pH 7 (0.1 and 0.25 w/w%) and pH 6 (0.5 w/w%), using microfluidizer.36

Figure 3.11 PSD plots of 0.1, 0.25 and 0.5 w/w% BB-LNPs-based emulsions, containing 5% RO or HD, prepared in 5 mM CA buffer at pH 7 using ultrasonication, at day 0, 7, and 14.....37

Figure 3.12 Representative pictures of the physical appearance and optical microscopy (100x magnification) of 0.1, 0.25 and 0.5 w/w% BB-LNPs-based emulsions, containing 5% RO or HD, prepared in 5 mM CA buffer at pH 7 using ultrasonication, at the day of preparation.37

Figure 3.13 PSD plots of 0.1, 0.25 and 0.5 w/w% PB-LNPs-based emulsions, containing 5% RO or HD, prepared in 5 mM CA buffer at pH 7 using ultrasonication, at day 0, 7, and 14.....38

Figure 3.14 Physical and microscopical characterization (with 40x and 100x magnifications) at 0 day of 0.1, 0.25 and 0.5 w/w% PB LNPs forming 5% RO and HD emulsions at pH 7.39

Figure 3.15 PSD plots of 0.1, 0.25 and 0.5 w/w% LB-LNPs-based emulsions, containing 5% RO or HD, prepared in 5 mM CA buffer at pH 7 using ultrasonication, at day 0, 6, and 14.....39

Figure 3.16 Physical and microscopical characterization (with 40x and 100x magnifications) at 0 day of 0.1, 0.25 and 0.5 w/w% LB LNPs forming 5% RO and HD emulsions at pH 7 with ultrasonication.....40

Figure 3.17. Global, bottom, and top TSI values for 0.1, 0.25 and 0.5 w/w% BB-LNPs-based emulsions, containing 5% RO or HD, prepared in 5 mM CA buffer at pH 7 using ultranication,

over 14 days.....	42
Figure 3.18 Global, bottom, and top TSI stability indicators for various ultrasonicated 5% RO and HD emulsions using 0.1, 0.25 and 0.5 w/w% LB LNPs of pH 7 at 0,7 and 14 days intervals.	42
Figure 3.19 Global, bottom, and top TSI stability indicators for various ultrasonicated 5% RO and HD emulsions using 0.1, 0.25 and 0.5 w/w% PB LNPs of pH 7 at 0,7- and 14-days intervals.	42
Figure 3.20 Phenolic content of 0.1, 0.25 and 0.5 w/w% LNPs-based emulsions (in three replicates), containing 5% RO or HD, prepared in 5 mM CA buffer at pH 7 using ultrasonication, at day 0.....	43
Figure 3.21 Antioxidant activity expressed in DPPH inhibition and mg AA eq/g lignin of 0.1, 0.25 and 0.5 w/w% LNP suspensions.....	45
Figure 3.22 Screening of bacterial inhibition of 0.5 w/w% of LB-, BB- and PB-LNPs at pH 6 against <i>Staphylococcus aureus</i> after 4 h contact compared with the control.	47
Figure 3.23 Screening of the bacterial inhibition after incubation of 0.5 w/w% of LB-, BB- and PB-LNPs at pH 6 against <i>E. coli</i> after 4 h contact compared with the control.....	48
Figure 3.24 Comparison of the grown colonies of 0.1 mL <i>Staphylococcus aureus</i> strains control (10^{-1} and 10^{-2}) and the counted colonies after 4 h contact inhibition of 0.1 mL 0.5 w/w% of BB-LNPs (10^{-1} and 10^{-2}) at pH 6 against <i>Staphylococcus aureus</i> . Abbreviations: NG: no growth, CFUs: colony forming units, HTBC: high to be count.....	50

List of tables

Table 1.1 Presence of the lignin monomers ratios from different natural sources.	15
Table 3.1 Span, $D_{3,2}$, and $D_{4,3}$ parameters' mean \pm SD values are listed for BB-LNPs at 0.1 w/w % concentration at 4 different optimization conditions. Statistical analysis was carried out by one-way analysis of variance (ANOVA) where unshared letters between each parameter' column is the significance value at $p \leq 0.05$	31
Table 3.2 Span, $D_{3,2}$, and $D_{4,3}$ parameters' mean \pm SD values are listed for BB-LNPs RO 5 mM CA microfluidizer at different conditions of pH and concentration. Statistical analysis was carried out by one-way ANOVA where unshared letters between each parameter' column is the significance value at $p \leq 0.05$	33
Table 3.3 Span, $D_{3,2}$, and $D_{4,3}$ parameters' mean \pm SD values are listed for PB-LNPs RO 5 mM CA microfluidizer at different conditions of pH and concentration. Statistical analysis was carried out by one-way ANOVA where unshared letters between each parameter' column is the significance value at $p \leq 0.05$	35
Table 3.4 Span, $D_{3,2}$, and $D_{4,3}$ parameters' mean \pm SD values are listed for BB-LNPs 5 mM CA ultrasonication at different conditions of oil and concentration. Statistical analysis was carried out by one-way ANOVA where unshared letters between each parameter' column is the significance value at $p \leq 0.05$	37
Table 3.5 Span, $D_{3,2}$, and $D_{4,3}$ parameters' mean \pm SD values are listed for PB-LNPs 5 mM CA ultrasonication at different conditions of oil and concentration. Statistical analysis was carried out by one-way ANOVA where unshared letters between each parameter' column is the significance value at $p \leq 0.05$	40
Table 3.6 Span, $D_{3,2}$, and $D_{4,3}$ parameters' mean \pm SD values are listed for LB-LNPs 5 mM CA ultrasonication at different conditions of oil and concentration. Statistical analysis was carried out by one-way ANOVA where unshared letters between each parameter' column is the significance value at $p \leq 0.05$	40
Table 3.7 Phenolic content of RO and HD for BB, PB and LB-LNPs-based emulsions expressed as mmol Van eq/g lignin (mean \pm SD) for different concentrations. Statistical analysis was carried out by one-way ANOVA where unshared letters between each LNPs' group is the significance value at $p \leq 0.05$	44
Table 3.8 Phenolic content of RO and HD for BB, PB and LB-LNPs-based emulsions expressed as mmol Van eq/L lignin (mean \pm SD) for different concentrations. Statistical analysis was carried out by one-way ANOVA where unshared letters between each LNPs' group is the significance value at $p \leq 0.05$	44

Table 3.9 Antioxidant activity for BB, PB and LB-LNPs-based emulsions expressed as mg AA eq/g lignin (mean \pm SD) for different concentrations. Statistical analysis was carried out by one-way ANOVA where unshared letters between each LNPs' group is the significance value at $p \leq 0.05$45

Table 3.10 Antioxidant activity for BB, PB and LB-LNPs-based emulsions expressed as DPPH inhibition % (mean \pm SD) for different concentrations. Statistical analysis was carried out by one-way ANOVA where unshared letters between each LNPs' group is the significance value at $p \leq 0.05$45

Table 3.11 Qualitative bacterial inhibition of 0.5 w/w% of LB-, BB- and PB-LNPs at pH 6 against *Staphylococcus aureus* and *E. coli* after 4 h contact compared with the control. LNPs inhibition results were compared relatively to the control.....48

Table 3.12. Quantitative results of bacterial inhibition of 0.5 w/w% of BB-LNPs at pH 6 against *Staphylococcus aureus* after 4 h contact compared with the control.....50

List of abbreviations

No.	Abbreviation	Description
1	LNPs	Lignin nanoparticles
2	CA	Citric acid
3	PSD	Particle size distribution
4	C-C	Carbon -carbon bond
5	w/w %	Weight/ weight percentage
6	mM	Millimole
7	TSI	Turbiscan stability index
8	BB	Hardwood birch
9	LB	Softwood kraft Lignoboost
10	PB	Alkali Protobind 1000
11	pH	Potential of hydrogen
12	SD	Standard deviation
13	mg	Milligrams
14	AA	Ascorbic acid
15	<i>E. coli</i>	<i>Escherichia coli</i>
16	h	Hour(s)
17	DPPH	2,2-diphenyl-1-picrylhydrazyl
18	Van	Vanillin
19	RO	Rapeseed oil
20	V _{final}	Final volume
21	W/O	Water in oil
22	HD	Hexadecane
23	Min	Minute
24	Sec	Second
25	SD	Standard deviation
26	V _{initial}	Initial volume
27	C _{initial}	Initial concentration
28	C _{final}	Final concentration
29	MQ-water	Milli-Q water
30	aq	Aqueous
31	THF	Tetrahydrofuran
32	rpm	Revolutions per minute
33	ANOVA	Analysis of Variance
34	UV/Vis	Ultraviolet/ visible
35	HTBC	High to be count
36	mmol Van eq/l	Millimole vanillin equivalent per liter
37	mmol Van eq/g	Millimole vanillin equivalent per gram
38	wt%	weight percentage
40		

List of symbols

No.	Symbol	Description
1	g	relative centrifugal force
2	$D_{3,2}$	Sauter diameter
3	$D_{4,3}$	Volumetric diameter
4	μ	Micro (10^{-6})
5	β	beta

Chapter 1: Introduction

1.1 Lignin background

Derived from lignocellulosic biomass, lignin is one component that represents *ca.* 15-30 % out of that mass and ranked as the second in abundance [1, 2] that is chemically composed of a cross-linked heteropolymer with an aromatic structure providing *ca.* 30% of organic carbon [3]. It consists mainly of three phenylpropanolic monomers that are referred as monolignols bonded together by C-C and ether bonds. As a plant constituent, lignin functions for water transportation and providing structure to plants [4, 5]. Given the above stated facts, it is the only expandable renewable feedstock composed of aromatic monomers for valorization purposes to design products with added value from lignin.

p-Coumaryl alcohol, coniferyl alcohol, and sinapyl alcohol are cinnamyl alcohol derivatives' monomers that compose lignin structure [6]. Also, these monomers can be referred by their root structure's names i.e., *p*-hydroxyphenyl (H), guaiacyl (G), and syringyl (S) (Figure 1.1). [7]

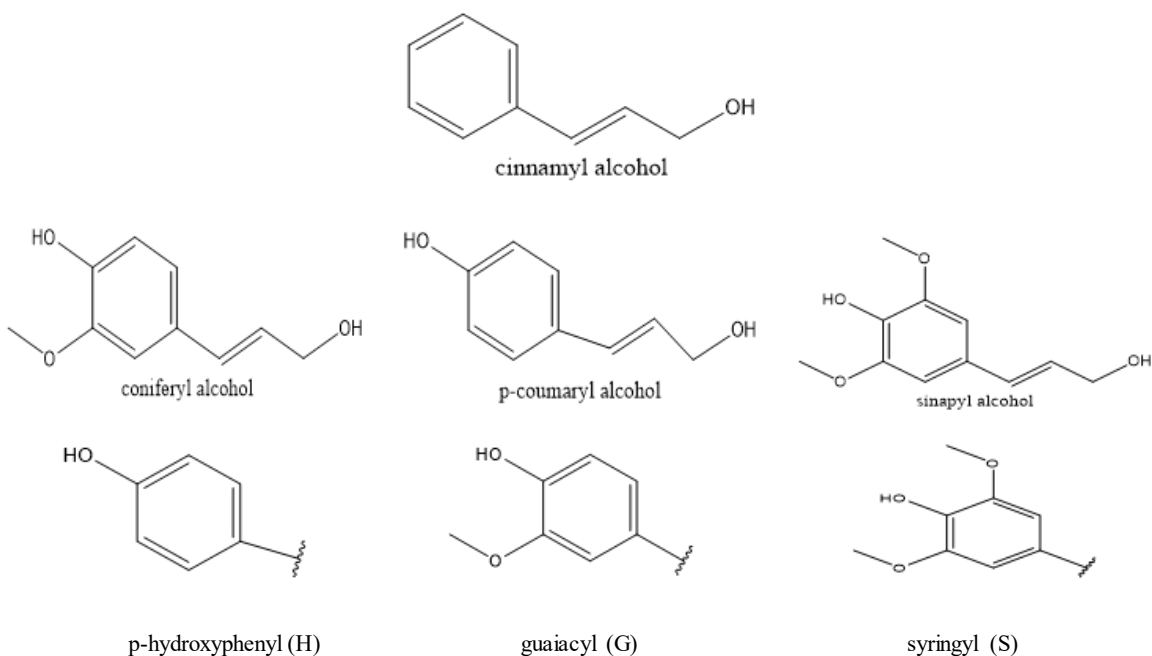


Figure 1.1 The main three cinnamoyl alcohol monomers present in lignin.

The ratio between units differs based on plant species or origin. For example, lignin found in grass consists of the three monomers, whereas the main monomer in softwood, represented in coniferous trees, is coniferyl alcohol and in hardwood is sinapyl alcohol [6] (Table 1.1). Consequently, with such variation in ratio of lignin units during polymerization, the formed bonds are different for instance, C-C bonding is more predominant in coniferous wood than deciduous wood [8]. Depending on the source from where lignin is isolated, these ratios differ, which can further impact both physicochemical and mechanical characteristics of lignin [6].

Table 1.1 Presence of the lignin monomers ratios from different natural sources.

Lignin source	Unit		
	coniferyl alcohol	sinapyl alcohol	p-coumaryl alcohol
Softwood	Present		
Hardwood	Present	Present	
Grass	Present	Present	Present

For the above-mentioned variation of both lignin units and bonds, it is challenging to draw the exact chemical structure for each isolated lignin owing to the complexity of the underlying polymerization process [7]. Polymerization of these lignin monomers that result in lignification occurs *in vivo* through enzymatic dehydrogenation forming C-C and ether bonds that leads to cross-linked amorphous lignin structure [9]. Lignin functions for transportation of water and other nutrients and protection against pathogens and insects is attributable to its hydrophobic nature. Among the natural bonds present in lignin structure, β -O-4 bonds were found dominating with almost 50% of all types of bonds and targeted to be broken for reactions as they are relatively easier than other existing bonds [10]. Figure 1.2

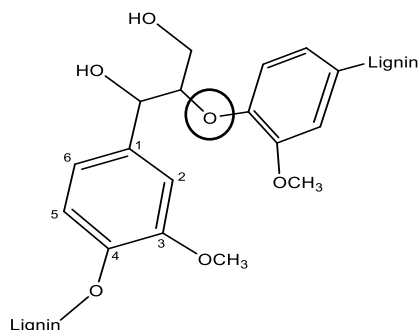


Figure 1.2 β -O-4 bond typical connection type in lignin's monomers highlighted in the black cycle.

1.2 Lignin isolation and depolymerization from biomass and types

Successful extraction processes of lignin from plant biomass requires considering some factors such as system pH, solvent/solute ratio, lignin fragmentation, lignin condensation prevention and lignin fragment dissolution. There are 4 typical methods used to isolate technical lignins, which are categorized into two main divisions based on the final outcomes of produced lignin's sulfur content, sulfur containing lignins and non-sulfur containing lignins[7].

Processes that produce lignin containing sulfur are sulfite and kraft, while those without sulfur are soda and organosolv [11]. Most of the produced lignin is processed using sulfite method with 1000 ton of lignin per year. In the sulfite process, a heated aqueous solution of sulphite or bisulfite salt with countercations such as Na^+ , NH_4^+ , Mg^{++} , or Ca^{++} are employed in the sulfite pulping [12]. The pH of the aqueous solution can range between 1 and 13.5 in proportion to cation type,

concentration, and solubility. The rate limiting reaction during sulfite delignification process is lignin aliphatic chain sulfonation. Depending on pulping solution pH, sulfonation reaction develops at different positions. The reaction ends up with a water-soluble lignosulfonate that can be solvated accompanying hemicellulose in the aqueous pulping liquor. To finalize lignin isolation from that liquor, additional steps such as precipitating, ultra-filtration, and fermentation can be employed.[7]

Kraft generated lignin, Lignin burned and employed for pulping mills as energy. In kraft process, depolymerization step occurs through fragments with higher solubility production owing to α and β ether bonds cleavage after adding NaOH and Na₂S mixture and heating at 165 °C. A minor amount of the lignin produced from this method was sulfated due to hydrosulfide anions presence while the remaining majority was sulfate-free allowing. Lignin isolation completed via acidification and precipitation. To enhance lignin isolation through Kraft approach, other technologies such as LignoBoost kraft technology where two steps of separation and washing occur allowing conditions optimization for each step producing high quality lignin can be merged and applied.[7]

Soda process, soda, is usually the method of choice for non-woody biomass supplies such as flax or sugar cane. Likewise, in kraft process, soda method begins with adding of NaOH(aq) followed by heating to around 160 °C. Soda depolymerization of lignin occurs also through breaking α and β ether bonds leading to free phenolic structures. Such formed fragments can be readily extracted upon acidification *via* precipitation from the pulping liquor. Compared to the sulfite process, soda method produces higher purity lignin with lower molecular weight[7].

As a non-sulfur containing lignin with industrial scale producing process, organosolv method has been implemented for lignin isolation. The method provides simultaneous biomass individual isolation of lignin, cellulose and hemicellulose streams. The method relies on heating aqueous-organic mixture of ethanol, methanol, acetone, or organic acids. Compared to previous methods, it lacks sulfur, high pressure and temperature considering it as environmental-friendly. However, due to the unoptimized material recover, organosolv approach is relatively higher in cost compared to the other three processes.

1.3 Lignin functional properties

There are several functional properties for lignin such as antioxidant, biodegradable, and its use in renewable materials [13]. Cross-linking and physical blending of lignin with other polymers leads to the production of various materials such as foams [14], adhesives [15, 16], thermosets [17, 18], and thermoplastics [19, 20]. Lignin different encompassed functional groups of methoxy, phenolic hydroxy and aldehyde [21, 22] supported its utilization in applications such as adhesives [23], xerogels, hydrogels [24].

Nevertheless, lignin attain limited valorization owing to lignin polydispersity, complexity and heterogenous chemical structure and irregular particles morphology that relays on both of extraction and source of lignin, its valorization has been limited.[25, 26] To overcome these obstacles, LNPs were recently developed to function as catalyst [27, 28], in drug delivery [29], in hydrogel's synthesis [30] and as biocidal neutralizing gram-positive and gram-negative bacteria [31] and to increase the antioxidant properties because of the increased specific surface area.[32] Moreover, Such LNPs stabilized Pickering emulsions for self-healing coating [33], microporous

foams [34], microcapsules [35, 36] and polymers which are molecularly imprinted due to its superior stability and chemical interfacial potential [37, 38].

For LNPs production, there have been several systems mentioned for example, pH shift [39], solvent exchange [40, 41], acid precipitation, polymerization, ultrasonication and crosslinking.[32, 42, 43] One limitation for these methods is the variability in morphology and homogeneity of the prepared particles that varies based on the grade of lignin and preparation method used. Such inconsistency reflects variable characteristics of solubility, molar mass, phenolic hydroxyl groups and purity.[32, 44, 45] Due to the versatility and the controlled particles sizes produced, solvent exchange approach, has increasingly been utilized [46, 47]. Solvent shifting produced LNPs' sizes above 100 nm [48, 49] and demanded water for dialysis process [38]. For example, various concentrations of lignin dissolved with tetrahydrofuran (THF) can result in LNPs size ranging from (200- 500 nm) after precipitating the lignin solution in water [50].

After obtaining LNPs, the particles maintain their ability to modify chemical structure owing to the presence of various functional groups such as phenolic and aliphatic OH and COOH and provide control for the morphology and polydispersity of lignin polymer [51, 52]. Therefore, lignin transformation into nanoparticles provides advantages of controlled morphological particles and applying them to act as carrier of drugs, stabilizers for emulsions [53-55], and antibacterial [51, 56] high value-added material.

Obtaining uniform size, smooth surfaces, and regular shape of produced LNPs is critical in achieving higher stability in formulations such as emulsions. Abovementioned properties are fulfilled with utilizing one common method, which is antisolvent precipitation. In this strategy of preparing LNPs, water acts as the antisolvent while several non-aqueous solvents can be used to dissolve the lignin, such as THF, dimethyl sulfoxide, ethanol, and acetone. As antisolvent precipitation, a 3:1 ratio of acetone/water is an effective, simple, cost-effective, environmentally-friendly and scalable strategy for preparing monodisperse homogenous, spherical and smooth surfaces of LNPs from three different lignins [45].

Due to the antioxidant, antifungal and antiparasitic properties ascribed to the phenolic hydroxy and methoxy groups, lignin can be utilized in food and foodstuffs as stabilizers [57-61]. Generally, lignocellulosic compounds are non-toxic, non-radioactive, odorless, and non-polluting materials [62] posing their use in food applications.

1.3.1 Emulsification

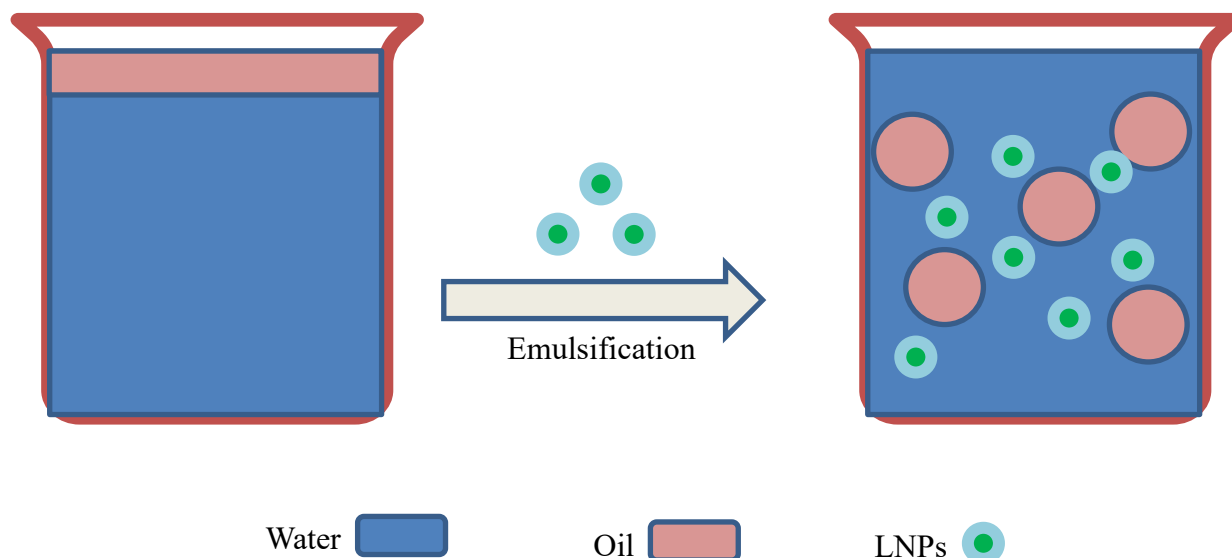


Figure 1.3 Figure shows simple representation of how emulsification of two immiscible liquids (water and oil) with the aid of the LNPs (emulsifying agent) occurs.

The term emulsion is defined as two immiscible liquids, one represents the external, continuous, or dispersing phase, and the other (dispersed, internal, or discontinuous phase) is dispersed in it such as, oil in water(O/W) emulsion (Figure 1.3). Typically, in food emulsified products, the mean diameter of the droplets constituting these emulsions falls between the range of 0.1 to 100 μm . [63]

O/W emulsions are predominant in food products, household, and utilized in pharmaceutical and agricultural industries [64]. Emulsion properties such as rheology, appearance and physical stability are strongly impacted by emulsion droplet size distribution. [65] PSD is dramatically affected by formulation of the emulsion, emulsification method and process variables [66]. Emulsification is usually aimed to produce smaller droplets as much as possible and obtain narrow PSD. Monodispersed emulsions contain same size of constituting droplets while in polydispersed ones, there are different droplet sizes. Therefore, several analytical techniques and experimentations can be applied to determine these characteristics. [63]

One of the processes that is needed for bringing the raw ingredient of emulsion (oil/ water) into an emulsion is homogenization. Homogenization process can be performed by implementing intense mechanical agitation force by the dedicated equipment (homogenizer). Equipment such as rotor-stator and high-pressure homogenizers are among the most common emulsifying devices. The mechanism of the rotor-stator homogenizer for the emulsifying process is by droplet breakup. While in case of high-pressure homogenizers, the high-pressure pumps force the emulsion course emulsion to pass through a narrow gap. Microfluidizers employ same mechanism of high pressure with a certain nozzle geometry and there is an interaction chamber based on microchannels. [64]

Considering that emulsions are thermodynamically unstable systems, there are four main manifestations of emulsion instability: sedimentation or creaming, coalescence, flocculation and Ostwald ripening. Sedimentation and creaming are the mechanisms where gravity affect dispersed droplet movement downwards if higher in density and upwards if lower in density, respectively. Coalescence is another mechanism where larger droplets are formed after fusion of smaller droplets. While flocculation occurs when aggregates of drops formed without emulsion interface rupture by sticking them together maintaining their integrity. In the Ostwald ripening, larger drops formed from the smaller drops. Such interactions are strongly dependent on emulsion droplet size.[63, 64]

Stabilizers can be incorporated into emulsions to avoid the thermodynamic emulsion instability of produced emulsion. These emulsifiers characterized as surface-active materials, can prevent droplet aggregations by forming coatings around these droplets. Moreover, it eases the homogenization step reducing the interfacial tension [63].

Without the vital role of stabilizers, oil and water normally do not form emulsion. As a key region subject to tension, the formed interfacial layer with stabilizer affects the emulsion structure. There are two main types of stabilizers, used in emulsions including synthetic and natural emulsifiers. An example of natural stabilizers is the lignocellulosic biomass with lipophilic/ hydrophilic content. Stabilizers are distributed throughout the emulsion where a portion constructs the interfacial layer between the two phases, while the other portion can be unabsorbed in the continuous phase [67-70].

In oil/water Pickering emulsions that use solid particles stabilizers alone, LNPs have been reported [53, 71, 72] to exert improved functionality as emulsifier in stabilizing mixed oil of isocyanate and 1-butyl-3-methylimidazolium hexafluorophosphate [BMIm]PF₆ as it produced an emulsion with stable droplets and uniform distribution of their sizes [73]. Moreover, incorporating LNPs as stabilizers in Pickering emulsions can be recycled using pH modification [74]. [38]

Recent studies showed the excellent emulsifying properties of LNPs due to its amphiphilic structure without adding extra surfactant. when measuring the stability of these LNPs-stabilized emulsion, TSI (Turbiscan stability index) values were found to be lower in to the presence of higher LNPs concentrations.[53]

The different lignin units can affect oil droplet stabilization, for examples, G unit had more clear function than S lignin for stabilizing oil droplet. Lignin units' abundance and types can affect droplet stabilization and its side groups with variable polarity can function in emulsion interface anchoring.[70]

The type of the stabilizing emulsifiers can impact long-term stability of emulsions. The choice of an emulsifier that suits a particular emulsion is dependent on several factors such as its minimum needed concentration, ability to prevent aggregation and produce small droplets[63].

1.3.2 Antibacterial

As for the natural polymers, lignin can be categorized as organic antimicrobial agents. Lignin structure contains various functional groups such as carbonyl, methoxy, phenolic and aliphatic hydroxyl groups that account for its antibacterial actions. As one of the functions in woody plants, lignin provide protection against microbial attack. Moreover, this function can be impacted by the origin and the extraction method used in lignin production, as the different technical lignin present

different properties. For example, kraft lignin with its high antioxidant and phenolic features showed higher antimicrobial effect against *E. coli*, *Staph aureus*, *Proteus mirabilis*, *Proteus vulgaris*, *Pseudomonas aeruginosa*, *Enterobacter aerogenes*, *Bacillus thuringiensis*, *Salmonella enterica serotype typhimurium* and *Streptococcus mutans* than commonly used antibiotics [62, 75-79].

Studies showed effectiveness of the unmodified lignin against gram-positive bacterial (*Bacillus sp.*) and gram-negative *Klebsiella sp.* The antimicrobial activity of lignin and containing composites with high amount of sugar was found active against both gram-positive and gram-negative bacteria [80, 81]. Therefore, in chemical, textile and food industries, protection against pathogenic microorganisms can be provided by employing lignin as antimicrobial additive [62].

1.3.3 Antioxidant activity

Sustainable use of resources, natural food additives, and consumer need for natural compounds in food industry to act as antioxidant replacing less safe synthetic ones is increasingly recognized [82]. Atoms, molecules, or ions with unpaired electrons having the tendency to gain or donate their electrons pairing together are referred to free radicals. These radicals represent a great threat for human health, because they are involved in aging, cardiovascular diseases, and cancer. Generally, thousands of free radicals and active oxygens are produced during metabolic processes and attack vital molecules such as DNA, lipids, carbohydrates, and proteins inside cells. Thus, scavenging these hazardous molecules will dramatically protect against several diseases [83-86].

Oxygen derived radicals exist either naturally in the atmosphere or are generated by processes of heating or irradiation of food and packaging. Such radicals initiate a series of reactions that lead to lipid oxidation. Therefore, eliminating such molecules from the food bulk represents an advantage, especially with naturally safe existing molecules containing the functional groups (phenolic structure) capable of capturing these radicals. Two factors can determine the efficiency of scavenging activity of antiradical, the rate of H atom abstraction from phenyl group and the stability of the produced phenoxy radical present in lignin aromatic structure (ArO●). The ability to scavenge free radicals (R●) of monomeric phenolic structure (existing in lignin) mainly relies on the mobility of H atom of the phenolic molecule (ArO-H) according to the below equation.



If there are any associated nonphenolic carbohydrate polymers, the concentration of phenolic OH groups will decrease leading to an increase in the bond strength connecting the O and H atoms of the phenolic OH dissociation enthalpy, and to negatively affect antioxidant reactivity [60, 61, 81, 87].

Chapter 2: Experimental section

In this work, three different lignocellulosic sources of BB, PB and LB lignins were used to prepare LNPs. The prepared LNPs were investigated for their emulsifying properties in O/W emulsion, antioxidant activity, phenolic content, and antibacterial effects as depicted in Figure 2.1.

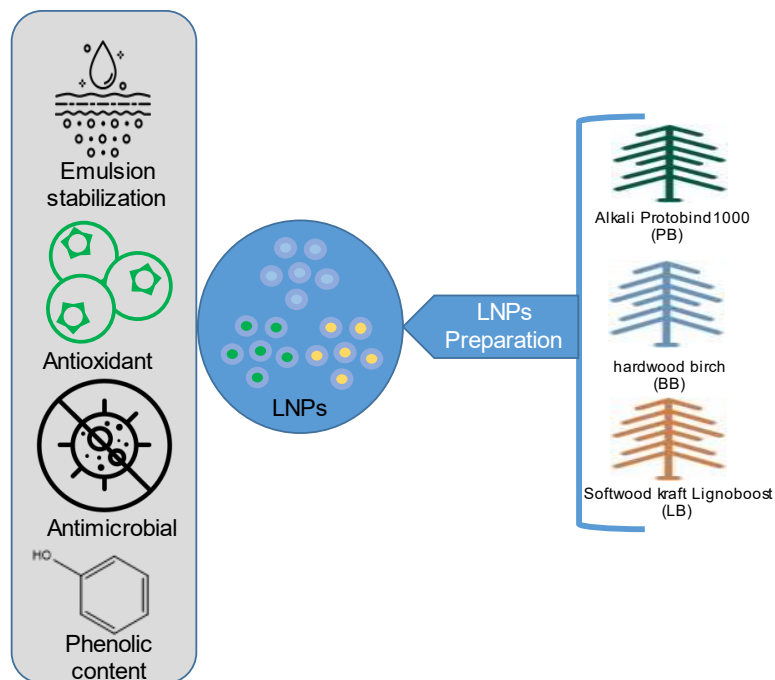


Figure 2.1 Diagrammatic flow of the major steps performed in this study including: LNPs preparation and testing their different functions of emulsifying, antibacterial, antioxidant properties and phenolic content.

1.1 Materials and methods

Three technical lignins from different lignocellulosic sources represented as softwood kraft Lignoboost (LB) supplied by Stora Enso (Finland), alkali Protobind 1000 (PB) isolated from wheat straw via a soda process (GreenValue SA, Switzerland), and BB isolated using the BLN process (CH Bioforce Oy, Finland). Acetone ($\geq 99.9\%$) was provided from Sigma Aldrich (Finland). Folin–Ciocalteu reagent, and Na_2CO_3 were purchased from Merck (Finland). Citric acid (CA) and rapeseed oil (RO) were provided from (Keiju, Bunge Finland Ltd, Raisio, Finland). n-Hexadecane (HD) was provided from Sigma Aldrich (Finland). Organisms used in antimicrobial assays were 787 *E. coli* (strain A), and 346 *Staphylococcus aureus* (strain B) strains purchased from DSMZ. Media used for microbial growth were Luria agar media and dilution buffer (Ringer), provided from Sigma Aldrich.

1.2 Preparation of LNPs

To prepare LNPs, 200mL of acetone/water (3:1) were mixed with 2 g of lignin and kept overnight with magnetic stirring. To remove undissolved solids, filtration through hydrophilic polypropylene membrane filters with a 0.7 μm pore size (Whatman) was followed. The filtrate was poured into 400 mL MilliQ-water to form the LNPs, under continuous stirring for 1 h. Further, using rotavapor under reduced pressure, residual acetone was removed followed by centrifugation for 15 min at 20000 rpm (50000g) of the LNPs suspensions, resulting in concentrated pellets of LNPs. The supernatant was discarded, and the LNPs were collected in a 50 mL glass breaker to obtain a concentrated LNPs suspensions. For redispersing the LNPs in solution, ultrasonication for 30 sec at 50% amplitude was done to obtain concentrated and dispersed LNPs suspensions. To determine the concentration of LNPs, 250 μl of LNPs dispersed solution was dried overnight using an oven set at 35 $^\circ\text{C}$. [45]

1.3 LNPs as an emulsion stabilizer

LNP concentrations of 0.1, 0.25 and 0.5 w/w% (weight/weight percentage) from each lignin were used as emulsifiers. LNPs were diluted with CA buffer to achieve the targeted final concentration, added to 5% of RO or HD, and the pH of the mixture was further adjusted to 6 or 7. The obtained emulsions were characterized using physical appearance, Master sizer 3000 (Hydro 3000 SM (Malvern Instruments Ltd, Worcestershire, UK), optical microscope (Carl Zeiss Axio Scope A1 (Zeiss, Oberkochen, Germany) and turbiscan (Lab Expert (Formulation, Toulouse, France). Figure 2.2.

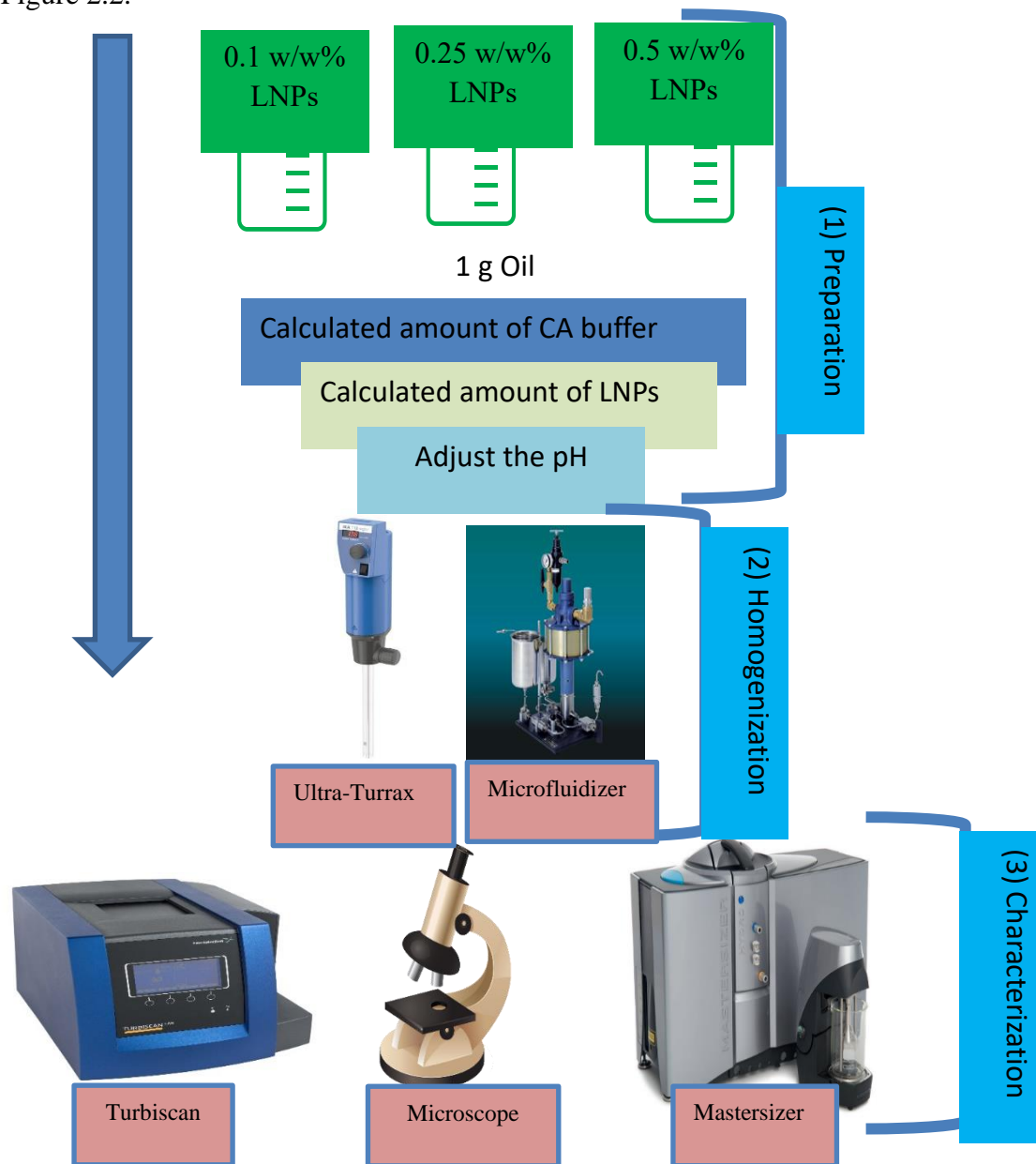


Figure 2.2 Diagrammatic sketch showing the steps of preparing emulsion, homogenization and its characterization.

1.3.1 Preparation of oil-in-water emulsions using microfluidizer

Initially, the LNPs and RO were added to CA buffers at different ionic strength and pH: 5mM (pH 5 and 7), 10 mM (pH 6 and 7) and 20 mM (pH 5).

formulation were mixed using an Ultra-Turrax (T-18 basic, IKA, Staufen, Germany) equipped with a disperser-type stirrer at 22000 rpm for 2 min to obtain a course emulsion, followed by microfluidizer (Microfluidizer 110Y, Microfluidics, Westwood, MA, USA) at 800 bar pressure for 4 total passes.

After attempting the different ionic conditions at different pH values, the optimized set condition to be followed for preparing LNPs-based emulsion using microfluidizer were 5mM CA at both pH 6 and 7. As described above, 5% O/W emulsions containing LNPs from PB, BB and LB (0.1, 0.25 and 0.5 w/w%) in 5mM CA buffer at pH 6 and 7 were prepared using Ultra-Turrax at 22000 rpm stirring for 2 min to obtain a course emulsion followed by microfluidizer at 800 bar pressure for 4 total passes.

1.3.2 Preparation of oil-in-water emulsions using ultrasonication

Similar conditions as described above were used to prepare emulsion using ultrasonication. After mixing the LNPs (0.1, 0.25 and 0.5 w/w%) and 5% of RO or HD (as alternative) in 5 mM CA buffer at pH 7, samples were subjected to ultrasonication at 30% amplitude for 7 cycles of 30 sec of sonication and 15 sec of pause. At the 4th cycle, samples were placed in an ice box. Figure 2.3

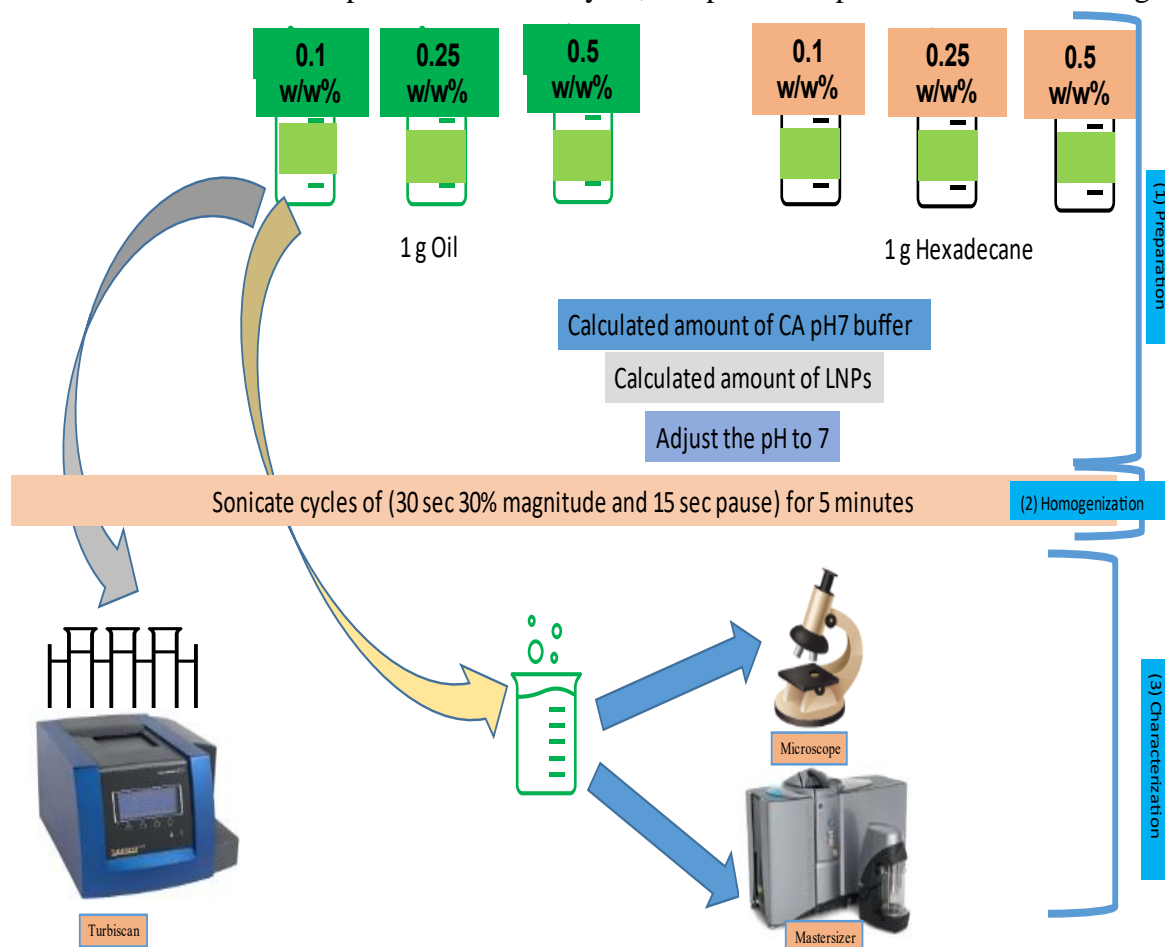


Figure 2.3 Diagrammatic flow chart showing steps of preparing, homogenizing, and characterizing 5% of RO and HD emulsions homogenized using ultrasonication by physical and microscopical examination, droplet size and stability.

1.3.3 Emulsion characterization

The prepared emulsions were characterized using these three main methods.

1.3.3.1 Optical Microscopy

Prepared emulsions were inspected under optical microscope at the day of preparation. Each sample was 10x diluted by adding 100 μl of the emulsion sample to 900 μl milliQ-water. One droplet of the preparation was placed onto glass slides, covered gently with glass coverslips, and checked under a Carl Zeiss Axio Scope A1 (Zeiss, Oberkochen, Germany) microscope using 40x and 100x magnification. Images were captured using Axio-vision Rel4.8 (Carl Zeiss, Germany) software using a built-in camera[70].

1.3.3.2 PSD characterization

Laser diffraction is one tool that can be employed to evaluate emulsion stability by PSD analysis over a period. Light scattering can monitor and characterize droplet sizes and migration change.

Mastersizer Hydro 3000 SM (Malvern Instruments Ltd, Worcestershire, UK) was utilized to evaluate DSD of the prepared emulsions using a static light scattering mechanism. Emulsion samples were carefully mixed, and small amount of the sample was drawn into MilliQ-water at each interval. A total of three measurement were generated for each sample analysis at several time intervals[70]. Stability storage intervals for prepared emulsion for optimizing ionic strength were up to 7 (PSD) and 14 (TSI) days, the duration for microfluidized homogenized emulsions was up to 30 days, and the ultrasonicated homogenized emulsion period was up to 14 days.

Measurements obtained from Laser diffraction using Malvern mastersizer 3000 generates droplet size distribution and droplet mean diameters data represented in $D_{3,2}$ (sauter diameter), $D_{4,3}$ (volumetric diameter) and Span (width of the distribution) and calculated as per the below equations. [88, 89]

$$D_{3,2} = \frac{\sum_{i=1}^N n_i d_i^3}{\sum_{i=1}^N n_i d_i^2}$$
$$D_{4,3} = \frac{\sum_{i=1}^N n_i d_i^4}{\sum_{i=1}^N n_i d_i^3}$$

Where d_i is the droplet diameter, n_i is the number of droplets having a diameter d_i , and N is the total number of droplets.

$$\text{Span} = \frac{D_{90} - D_{10}}{D_{50}}$$

Where each D_{90} , D_{10} and D_{50} represents the size of the particle below which 90%, 10%, and 50% of the sample lies, respectively.

$D_{4,3}$ indicates the presence of the large particles while $D_{3,2}$ is related to the small particles. Higher difference between the two diameters means the distribution of the particle sizes is bimodal with two peaks. However, when the two values are close together, it reflects the presence of one peak only. [88]

1.3.3.3 Emulsion stability kinetics

For stability assessment of the prepared and stored emulsions over time, Turbiscan Lab Expert (Formulaction, Toulouse, France) was employed to scan emulsion layers at 800 nm wavelength. It detects and quantifies destabilization activities for emulsions under investigations. In the Turbiscan, there is a light source and two detectors, transmission, and backscattering detectors. Emulsion under testing is put into the measurement position followed by scanning process along emulsion containing tube height

The software generates TSI values based on combining transmitted and backscattered light intensities. These values can be presented in terms of global (overall emulsion height), bottom (lower part) and top (upper part). Similarly to Mastersizer, measurements were performed at different intervals depending on the study duration [70].

Emulsion under testing is placed into the measurement position followed by scanning process along emulsion containing tube height. To study the change of stability over time, other repeats with same manner at the intended intervals can be performed and data compared to check the change over that certain duration. Turbiscan stability index (TSI) values can be extracted from the device to reflect the emulsion stability or instability. To evaluate different emulsions or same at different intervals, lower TSI values indicates better physical stability and vis-versa.[64]

1.4 Antibacterial effects of LNPs

E. coli, and *Staphylococcus aureus* suspensions were obtained by taking one separate fresh colony from each strain into 1 mL of Ringer solution. From the prepared bacterial suspensions, 100 μl of each strain was introduced into sterile Eppendorf tubes, each containing 900 μl of 0.5 w/w LNPs sample concentration and denoted as 10^{-1} with bacterial name and LNPs present. Similarly, 100 μl of both bacterial strain suspensions were added into 900 μl of Ringer solution acting as a control and labeled as 10^{-1} with name or the bacteria used. The tubes containing both control organisms and sample treatments were incubated for a contact time of 4 h at 37 °C. After incubation, serial dilutions from each of the resulted (10^{-1}) sample and control suspensions were attempted until 10^{-5} dilution. A preliminary screening test was performed to investigate the inhibition level of the three LNPs at 0.5 w/w% in 5mM CA buffer pH 6. From each level (10^{-1} to 10^{-5}) of each LNPs sample (LB-, PB-, and BB-LNPs) and control (*E. coli*, and *Staphylococcus*), A 10 μl was withdrawn and inoculated in triplicates onto Luria agar media. Figure 2.4

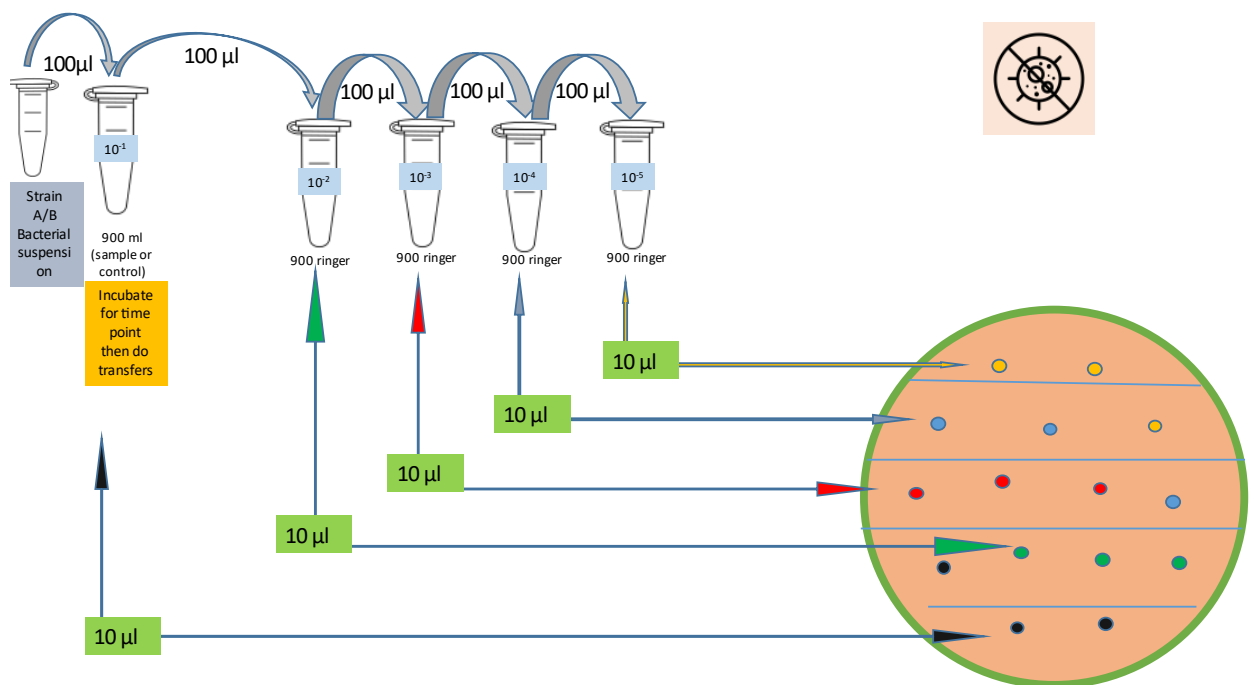


Figure 2.4 Diagram showing the general outline to screen bacterial inhibition of 0.5 w/w% of LB-, BB- and PB-LNPs around against *E. coli*, and *Staphylococcus aureus* strains. Each colored three cycles indicate the three replicates of different level of dilution to be screened.

After the preliminary screening, extra assays were attempted to determine how many logs of reduction occurred. Similar to the above-mentioned description of testing, the sequence of the steps was performed; however, the final amount withdrawn from the Eppendorf was 100 µl not 10 µl to be plated onto one plate using surface spread technique for both *Staphylococcus aureus* not *E. coli*. (Figure 2.5) After incubating these plates at 37 °C for 24 h, the colonies were counted and the difference in log reduction between the samples and the control was calculated indicating the inhibition efficiency of the lignin samples against *Staphylococcus aureus* by the following equation.

$$\text{Log reduction} = \text{Log} \frac{\text{control}}{\text{sample}}$$

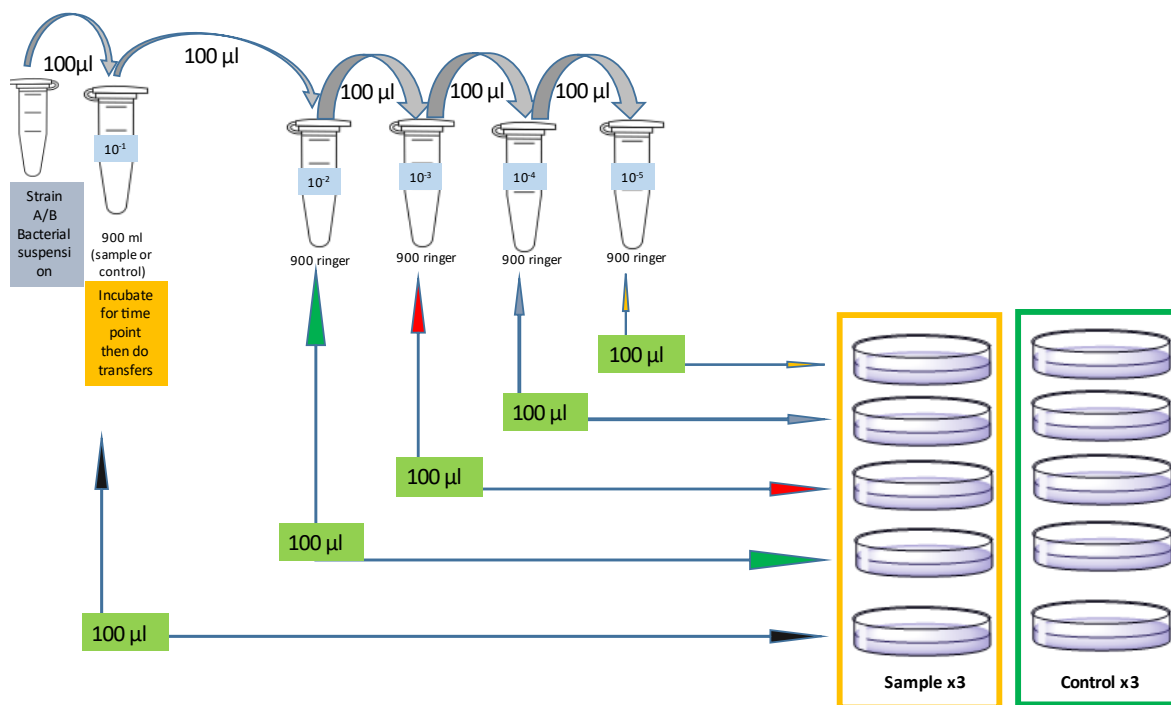


Figure 2.5 A diagrammatic sketch simplifies the steps to screen and identify number of bacterial logs of inhibition generated by BB LNPs against *Staphylococcus aureus* strain. The plates were plated using surface spread technique in triplicates after incubation.

1.5 Total phenolic content of LNPs-based emulsions

For measuring the phenolic content of the prepared LNPs-based emulsions, UV-Vis spectroscopy technique was used based on Folin-ciocalteu reagent, which interact with phenolic groups present in lignin structure reflecting the intensity of the phenolic component at 760 nm wavelength [90]. Vanillin (Van) acted as a standard due to its structural similarity with main lignin monomers units. **Error! Reference source not found..**

For that, 50 µl of the three lignin-based emulsions was diluted in 1.8 mL of MilliQ-water, and mixed with 150 µl of Folin-ciocalteu reagent. Then, 500 µl of 20 w/w% Na₂CO₃ solution were added, and the suspensions were shaken in a water bath at 40°C for 30 min. After the incubation, the absorbance at 760 nm of the developed blue colored samples was measured using UV/Vis spectrophotometer (UV-1800 Shimadzu).

1.6 Antioxidant activity of LNPs

Several antioxidant assays have been developed for measuring antioxidant potential of natural substances including DPPH in vitro based assay also reported for assessing lignin antiradical properties[83-86].

LNPs were tested for their antioxidant properties against 2,2-diphenyl-1-picrylhydrazyl (DPPH), using ascorbic acid (AA) as standard, in 96-well plates. The blank sample consisted of 300 µl of methanol and MilliQ-water in a 1:1 ratio, and DPPH control contained 150 µl of DPPH (200 µM) added to 150 µl of MilliQ-water. For the standard, 150 µl of AA was used in a series of concentrations, while for each sample, 150 µl of LNP suspensions was added to each well. Then, the absorbance was measured at 517 nm wavelength to obtain the background values, using a Varioskan plate reader (Thermo Fisher Scientific Inc., USA). After that, 150 µl of DPPH (200 µM) was added to each well, and incubated for 30 min in a dark room temperature condition. A second

measurement for the absorbance at 517 nm using the variokan plate reader was done to observe the difference.

The DPPH inhibition percentage was then calculated based on the following equation.

$$\text{DPPH inhibition \%} = \frac{A_{\text{control}} - A_{\text{sample}}}{A_{\text{control}}} \times 100$$

where A_{control} is the absorbance of the control reaction and A_{sample} is the absorbance of the sample. [91]

Chapter 3: Results and discussion

1.1 LNPs as an emulsion stabilizer

1.1.1 Optimization of LNPs in different ionic strengths and pH

As part of the conducted comparative study, different parameters, such as pH and ionic strength, were set and optimized to formulate LNPs-based emulsions with high stability and small and uniform PSD values. After examining the effect 5, 10 and 25 mM CA buffers with variable pH ranging from 5 to 7, the obtained results were also variable. Developed emulsions with 25 mM CA buffer at pH 5 exhibited an emulsion phase separation, while those prepared with 5 and 10 mM CA buffers produced better preparation in physical appearance without emulsion breaking. When testing the impact of pH change in the emulsions prepared with 5 or 10 mM CA buffers, the emulsions prepared at pH 7 were better than pH 5 or 6 in physical appearance, as a coarse layer was formed at pH 5 (Figure 3.1). Checking the PSD values of the same emulsions, peaks at around and higher than 100 μm were observed at pH 5 (Figure 3.2). For the set carried out at pH 7, almost uniform peaks appeared around 1 μm size. These data suggested that optimized outcomes can be aimed with neutral pH and lower ionic strengths. In addition, the stability checked over a week expressed in PSD values was not impacted as the peaks of each interval were almost overlapping over the initial peaks with a slight variation in the intensity. Also, TSI values in Figure 3.3 suggested similar optimization pattern as in PSD, with lowest TSI value for 5 mM CA pH 7, showing higher stability compared to the other formulations. Moreover, span, $D_{3,2}$, and $D_{4,3}$ parameters were calculated and listed in Table 3.1. Such variant data suggested possible reactions that might occur in lignin structure at higher ionic strengths or lower pH values, rendering the particles to aggregate leading to phase separation and emulsion instability.[63] Taking into account this preliminary screening, the data generated suggested that 5 mM CA buffer at pH 6 or 7 were optimal to compare the impact of different LNPs' sources and concentrations as emulsifiers.

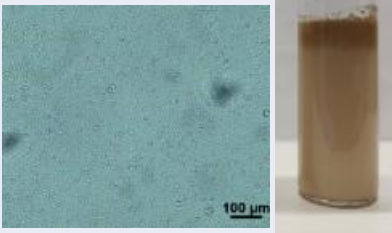
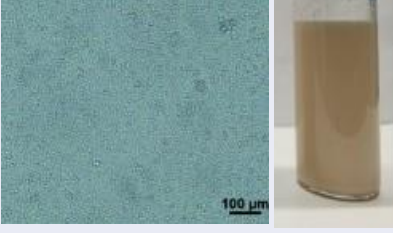
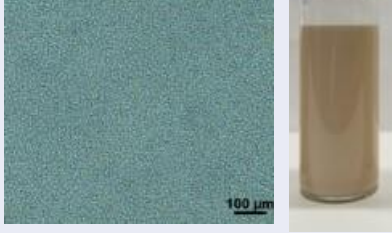
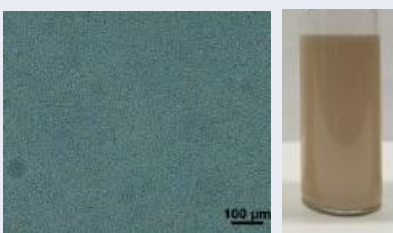
0.1 w/w BB-LNPs ionic and pH trial	5 mM CA	10 mM CA
pH	5	6
40x		
pH	7	7
40x		

Figure 3.1 Representative pictures of the physical appearance and optical microscopy (40x magnifications) of 0.1 w/w% BB-LNPs-based emulsions, containing 5% RO, prepared in 5 and 10 mM CA buffer at pH 5, 6 and 7 using microfluidizer, at the day of preparation.

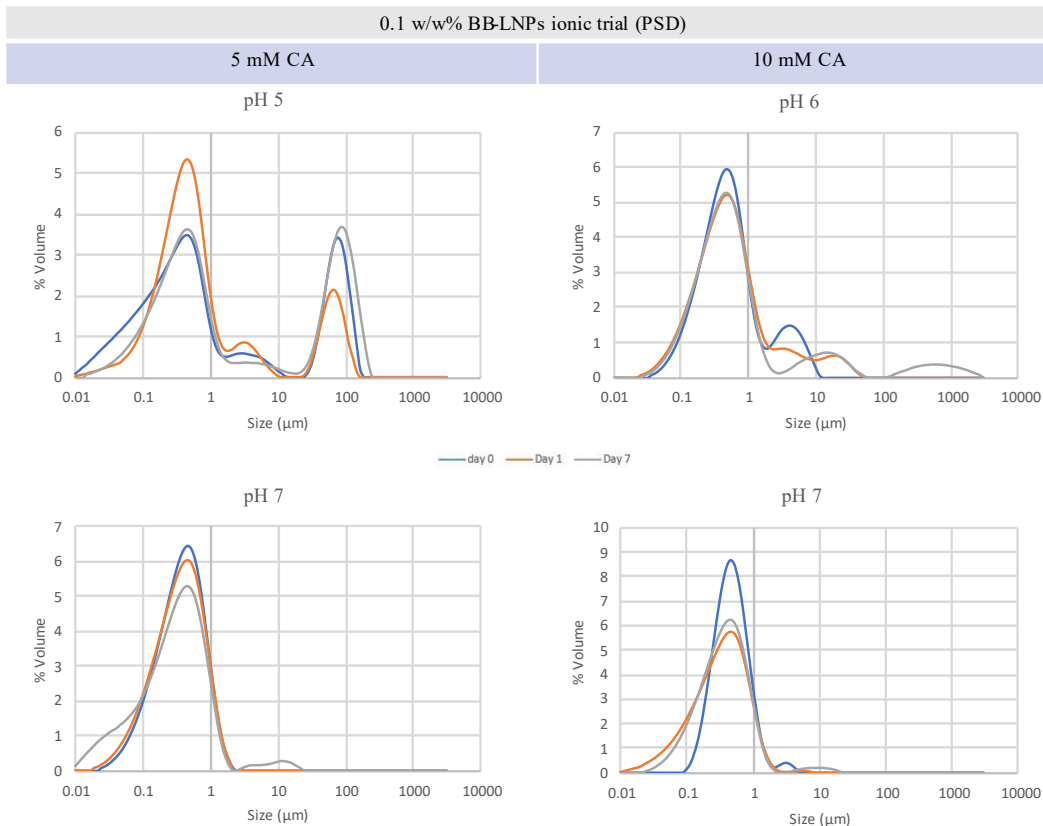


Figure 3.2 PSD graphs for 0.1 w/w% BB-LNPs-based 5% RO emulsions, at different ionic strengths and pH at day 0, 1 and 7.

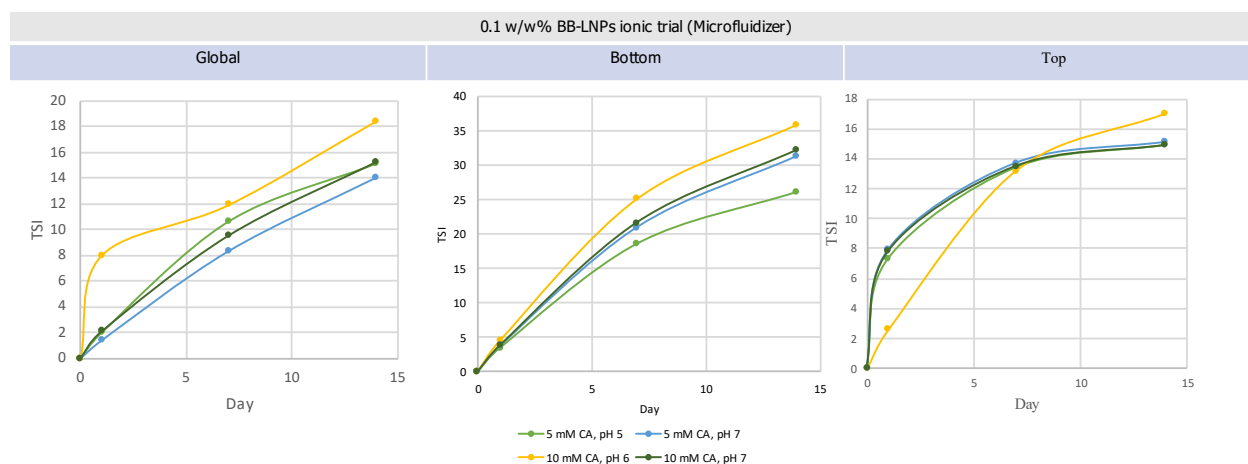


Figure 3.3 TSI values indicating the stability of 0.1 w/w% BB-LNPs-based 5% RO emulsions prepared with different ionic strengths (5 and 10 mM CA buffers) and pH 5, 6 and 7, at different height levels (global, bottom, and top) over 14 days.

Table 3.1 Span, $D_{3,2}$, and $D_{4,3}$ parameters' mean \pm SD values are listed for BB-LNPs at 0.1 w/w % concentration at 4 different optimization conditions. Statistical analysis was carried out by one-way analysis of variance (ANOVA) where unshared letters between each parameter' column is the significance value at $p \leq 0.05$.

Samples	Optimization (BB-LNPs 0.1 w/w %)		
	Span	$D_{3,2}$ (μm)	$D_{4,3}$ (μm)
5 mM CA pH 5	1253.881485 \pm 1011.655 ^a	0.262767 \pm 0.151799 ^a	22.83333 \pm 7.651362 ^a
10 mM CA pH 6	18.70778575 \pm 0.713084 ^a	0.346 \pm 0.001 ^a	1.146667 \pm 0.020817 ^b
5 mM CA pH 7	4.784803709 \pm 0.033436 ^a	0.251 \pm 0 ^a	0.477333 \pm 0.001155 ^b
10 mM CA pH 7	2.380454382 \pm 0.01624 ^a	0.425333 \pm 0.000577 ^a	0.619667 \pm 0.000577 ^b

1.1.2 Preparation of oil-in-water emulsions using microfluidizer

After determining the optimized parameters for emulsion development, the three LNPs sources (BB, PB and LB) were used in different amounts (0.1, 0.25 and 0.5 w/w%) to prepare 5% RO in 5 mM CA buffers at pH 6 and 7 using microfluidizer.

For the BB-LNPs initial PSD measurement, aside from the peak below 1 μm , the set performed at pH 6 showed a distinct peak around 100 μm for LNP concentrations of 0.25 and 0.5 w/w% and another broad peak from 5 to 50 μm at 0.1 w/w% LNPs. However, for the set carried out at pH 7, the PSD values were all optimum with almost symmetrical shape below 1 μm size (Figure 3.4). This suggested the effect of the increased acidity in developing larger particles. Such difference between the two sets was reflected also in the physical appearance of emulsions at pH 6, where a small layer of course particles was present at the top of the emulsion compared to pH 7 (Figure 3.5).

Upon evaluating the stability of BB-LNPs-based emulsions after storage for 30 days, their PSD values were less variable with smaller peaks over 100 μm at pH 7 than at pH 6, which showed more variable and larger peaks ranging from 10 to over 1000 μm . Additionally, TSI values supported the idea of more stabilized emulsions at pH 7 with lower TSI values compared to those at pH 6 over a week storage. Relating concentration to stability, results revealed higher stability reflected on lower TSI values in response to higher concentrations of LNPs during storage. Moreover, the stability of 0.5% BB-LNPs-based emulsions at pH 6 was higher than those containing 0.1% LNPs at pH 7 (Figure 3.6). Moreover, span, $D_{3,2}$, and $D_{4,3}$ parameters were calculated and listed in Table 3.2. These results indicated that higher concentration of LNPs could compensate for the lower pH condition needed to stabilize emulsions. Lignin can provide steric stabilization of emulsions not only due to its aromatic web shaped hydrophobic structure and hydrophilic chains but also due to their nanoparticles properties of high surface activity and spherical particles [70]. Destabilization of emulsion can be impacted by the emulsifier's concentration. At lower concentration, the amount of emulsifier might not be sufficient to fully cover the surface of the droplets, leading to flocculation and/or coalescence. TSI values can indicate emulsion destabilization, where high values reflect high instability. [92]

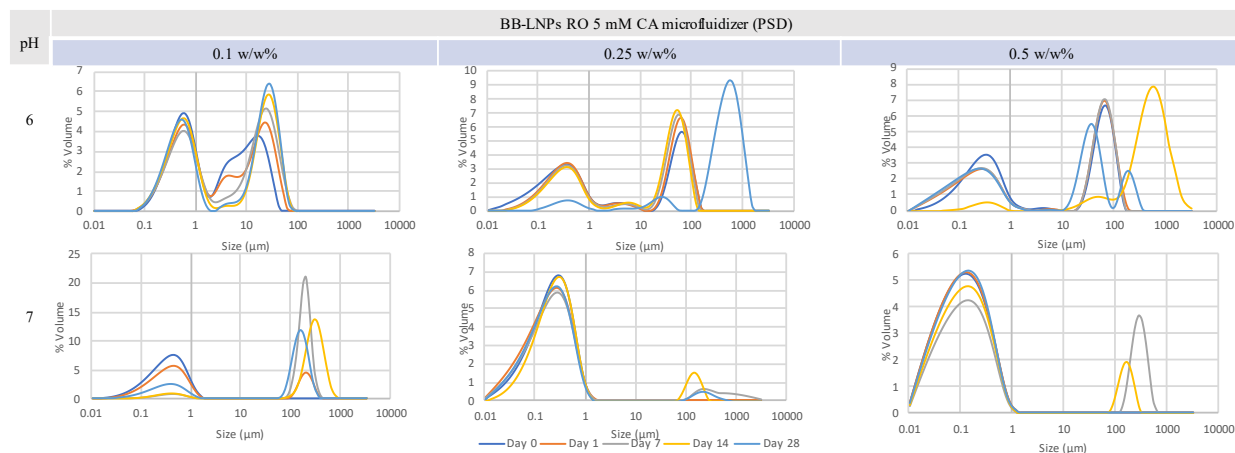


Figure 3.4. PSD plots of 0.1, 0.25 and 0.5 w/w% BB-LNPs-based emulsions, containing 5% RO, prepared in 5 mM CA buffer at pH 6 and 7 using microfluidizer, at day 0, 1, 7, 14, and 30.

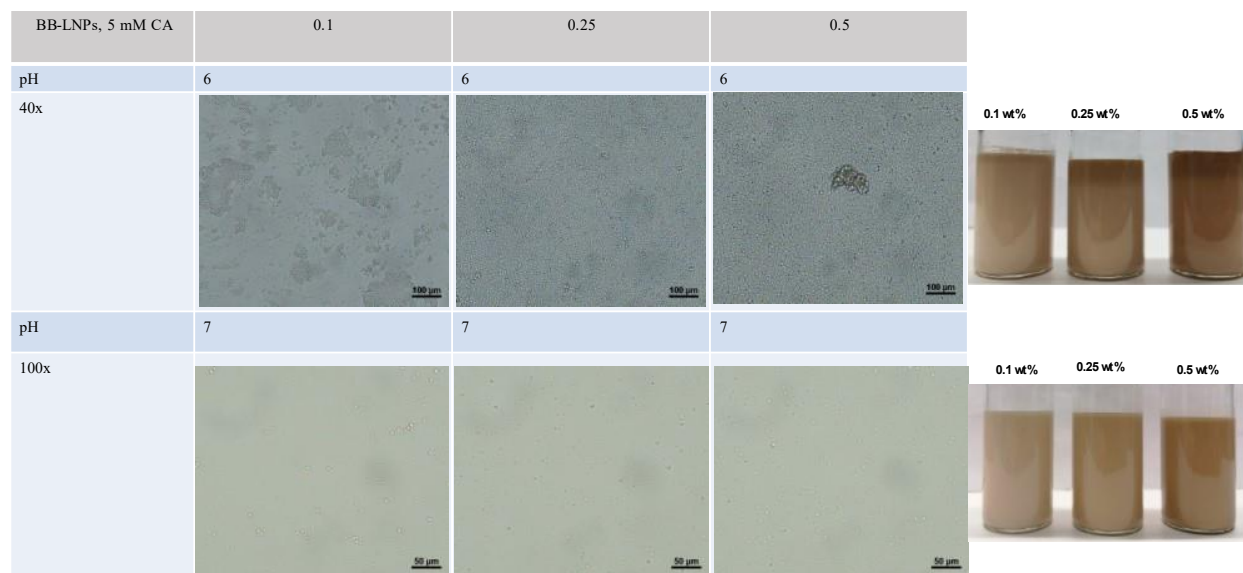


Figure 3.5 Representative pictures of the physical appearance and optical microscopy (40x and 100x magnifications) of 0.1, 0.25 and 0.5 w/w% BB-LNPs-based emulsions, containing 5% RO, prepared in 5 mM CA buffer at pH 6 and 7 using microfluidizer, at the day of preparation.

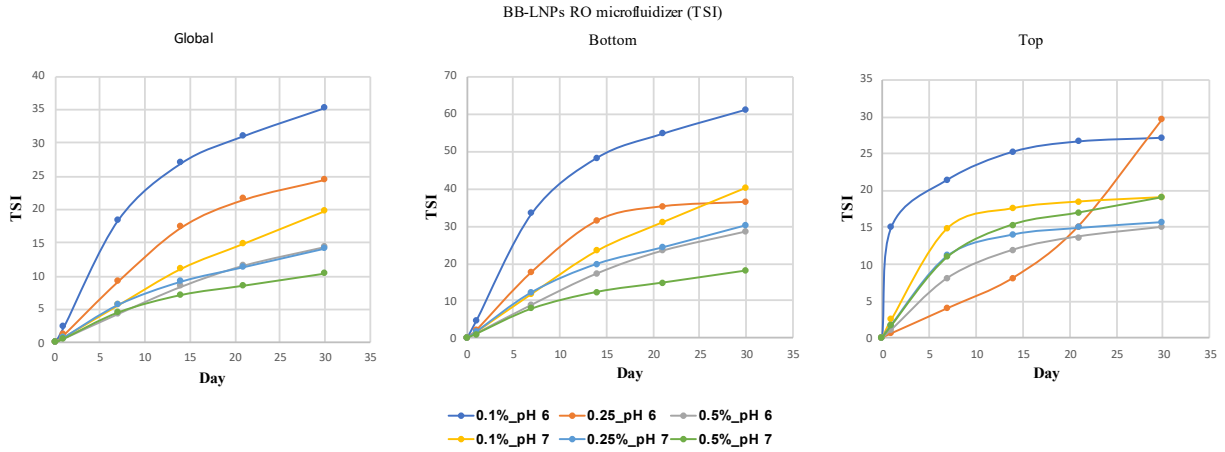


Figure 3.6 Global, bottom, and top TSI stability values for 0.1, 0.25 and 0.5 w/w% BB-LNPs-based emulsions, containing 5% RO, prepared in 5 mM CA buffer at pH 6 and 7 using microfluidizer, over one month.

Table 3.2 Span, $D_{3,2}$, and $D_{4,3}$ parameters' mean \pm SD values are listed for BB-LNPs RO 5 mM CA microfluidizer at different conditions of pH and concentration. Statistical analysis was carried out by one-way ANOVA where unshared letters between each parameter' column is the significance value at $p \leq 0.05$.

Samples	BB-LNPs RO 5 mM CA microfluidizer		
	Span	$D_{3,2}$ (μm)	$D_{4,3}$ (μm)
0.1 w/w% pH 7	$5.134203397 \pm 0.019727^b$	$0.201333 \pm 0.000577^{bcd}$	0.399667 ± 0.000577^b
0.25 w/w% pH 7	$6.901078325 \pm 1.636555^b$	0.125 ± 0.018193^{cd}	0.282667 ± 0.016166^b
0.5 w/w% pH 7	10.95419847 ± 0^b	0.0645 ± 0^d	0.167 ± 0^b
0.1 w/w% pH 6	$61.59800905 \pm 2.349786^b$	0.711 ± 0.016093^a	6.076667 ± 0.083267^b
0.25 w/w% pH 6	$975.2768911 \pm 654.9142^a$	0.302667 ± 0.154173^b	27.9 ± 6.823489^a
0.5 w/w% pH 6	$703.9316928 \pm 151.6412^a$	$0.275333 \pm 0.024173^{bc}$	30.56667 ± 4.461315^a

For PB-LNPs source stabilizers, both conditions at pH 6 and 7 showed one peak at less than $1\mu\text{m}$ PSD, and physically they were more uniform emulsions. Analyzing PB-LNPs homogenized emulsion stability, almost all samples showed consistency in PSD during the storage period up to 14 days (. Similarly, as in BB-LNPs preparation, higher concentration of 0.5 % LNPs stabilizer in both pH conditions supported their emulsions for the whole month with small peak at pH 7 more than lower concentrations of 0.1 and 0.25 w/w% LNPs

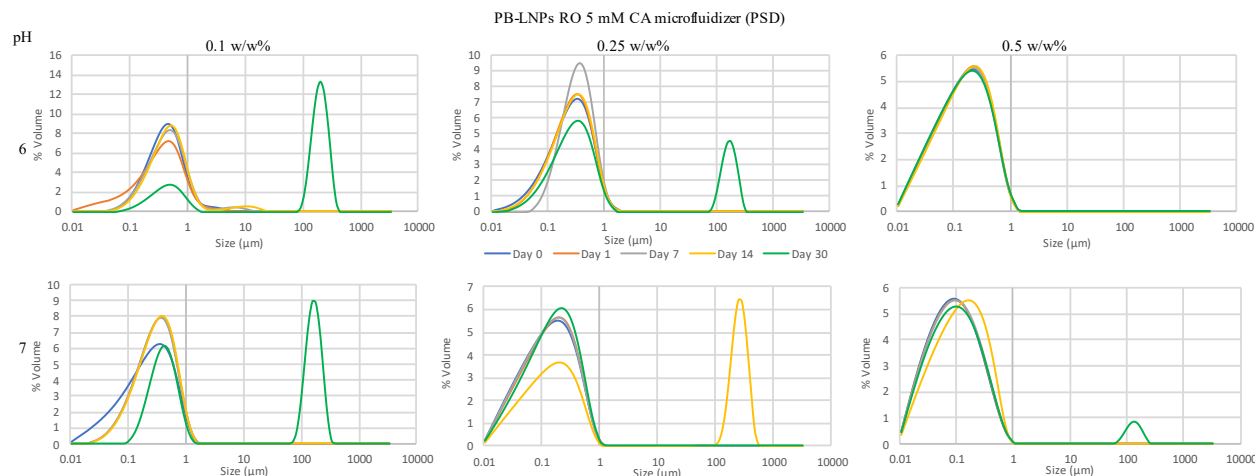


Figure 3.7 and Figure 3.8). Assessing TSI values for PB-LNPs, emulsions with pH 7 showed lower values (higher stability) than in pH 6 with exception 0.5 w/w% LNPs of pH 6 (Figure 3.9). Moreover, span, $D_{3,2}$, and $D_{4,3}$ parameters were calculated and listed in Table 3.3. Likewise, both higher pH and concentration provided optimum conditions for nearly steady and uniform formulations.

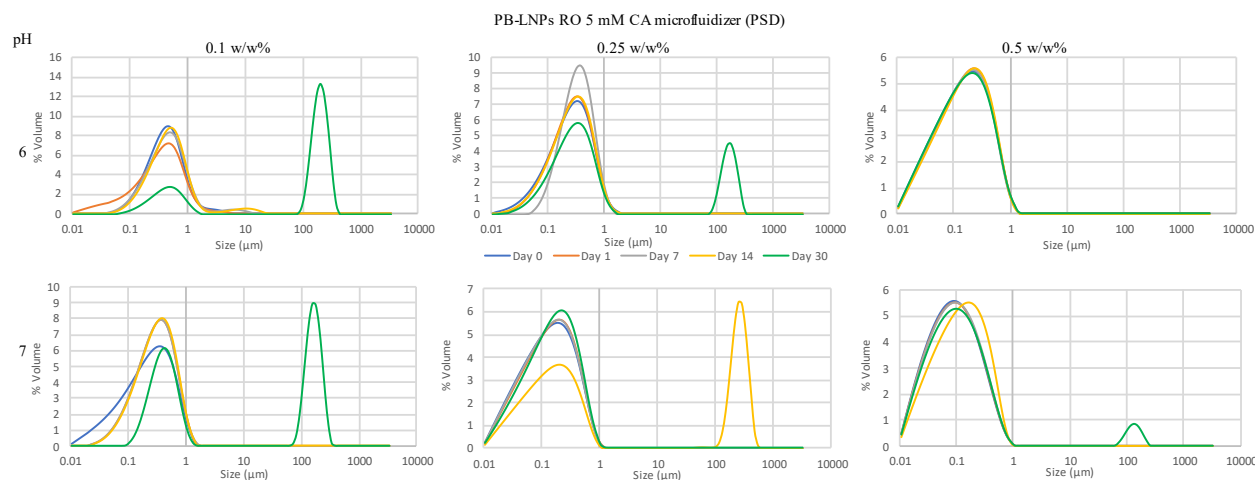


Figure 3.7 PSD plots of 0.1, 0.25 and 0.5 w/w% PB LNPs forming 5% RO emulsions at pH 6 and 7 using microfluidizer at 0, 1-, 7-, 14-, and 30-days intervals.

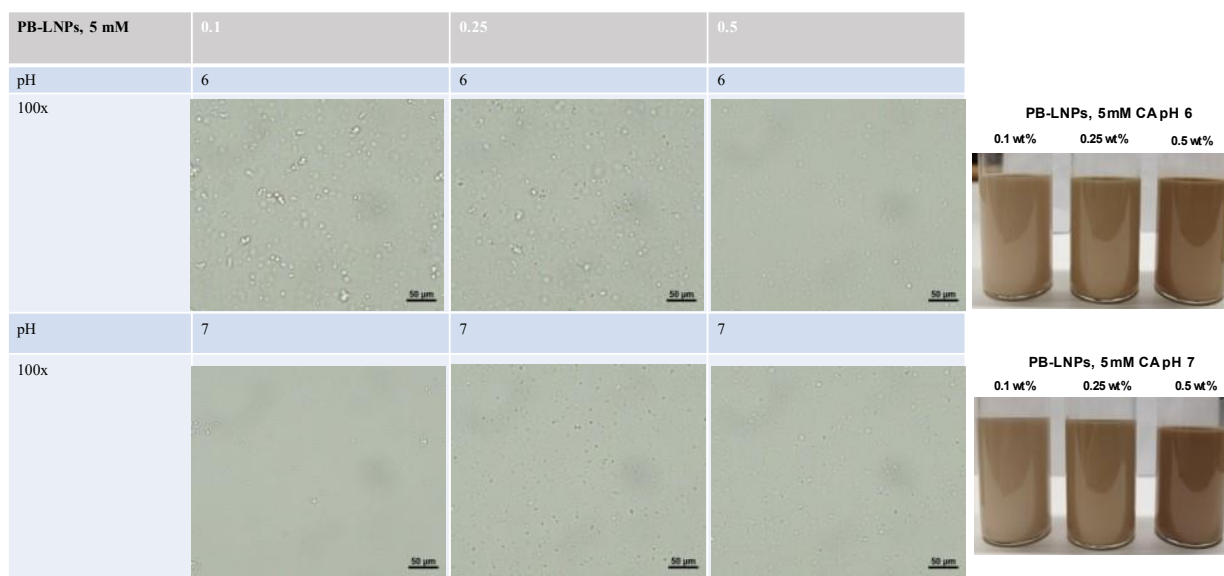


Figure 3.8 Representative pictures of the physical appearance and optical microscopy (100x magnifications) of 0.1, 0.25 and 0.5 w/w% PB-LNPs-based emulsions, containing 5% RO, prepared in 5 mM CA buffer at pH 6 and 7 using microfluidizer, at the day of preparation.

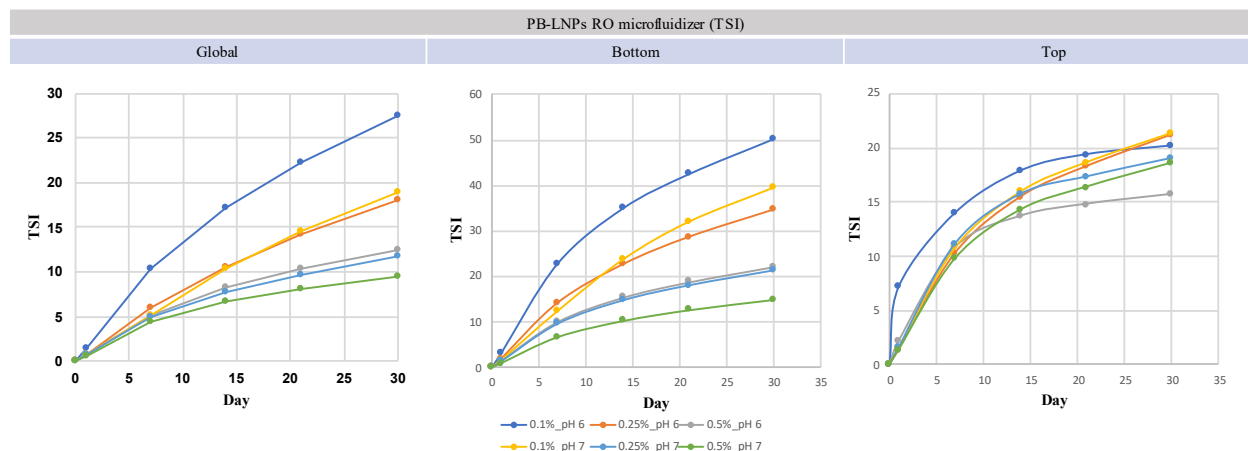


Figure 3.9 Global, bottom, and top TSI stability indicators for various formed 5% RO emulsions using 0.1, 0.25 and 0.5 w/w% BB LNPs at pH6 and 7 over a month duration interval.

Table 3.3 Span, $D_{3,2}$, and $D_{4,3}$ parameters' mean \pm SD values are listed for PB-LNPs RO 5 mM CA microfluidizer at different conditions of pH and concentration. Statistical analysis was carried out by one-way ANOVA where unshared letters between each parameter' column is the significance value at $p \leq 0.05$.

Samples	PB-LNPs RO 5 mM CA microfluidizer		
	Span	D _{3,2} (μm)	D _{4,3} (μm)
0.1 w/w% pH 7	9.430108005 ± 4.899013 ^a	0.133367 ± 0.066178572 ^{bc}	0.306667 ± 0.053529 ^b
0.25 w/w% pH 7	10.36552478 ± 0.034437 ^a	0.074933 ± 0.00011547 ^{cd}	0.194 ± 0 ^c
0.5 w/w% pH 7	9.556497175 ± 0.002446 ^a	0.056 ± 0 ^d	0.134 ± 0 ^d
0.1 w/w% pH 6	3.430987945 ± 0.011055 ^b	0.315333 ± 0.00057735 ^a	0.535667 ± 0.002082 ^a
0.25 w/w% pH 6	5.714290444 ± 0.011212 ^{ab}	0.153 ± 0 ^b	0.325667 ± 0.000577 ^b
0.5 w/w% pH 6	11.18503375 ± 0.031226 ^a	0.080633 ± 0.00005773 ^{bcd}	0.22 ± 0.001 ^c

Comparing both PB and BB lignin types as stabilizers, although PB showed better results on the preparation and over time after storage, the differences were not high, especially at pH 7. On the other hand, using LB-LNPs as stabilizers, the results were not successful as they showed broken/phase separated emulsions at both pH 6 and 7 (Figure 3.10). This suggested that the structure and composition of LB-LNPs can exert an impact during the emulsion preparation, forming larger and more coarse particles compared to BB-LNPs and PB-LNPs-based emulsions. Such results directed the experimental design of the study to introduce new parameters, such as implementing a different technique of emulsification and adding another alternative to RO to obtain reduced particle size and uniform emulsions.

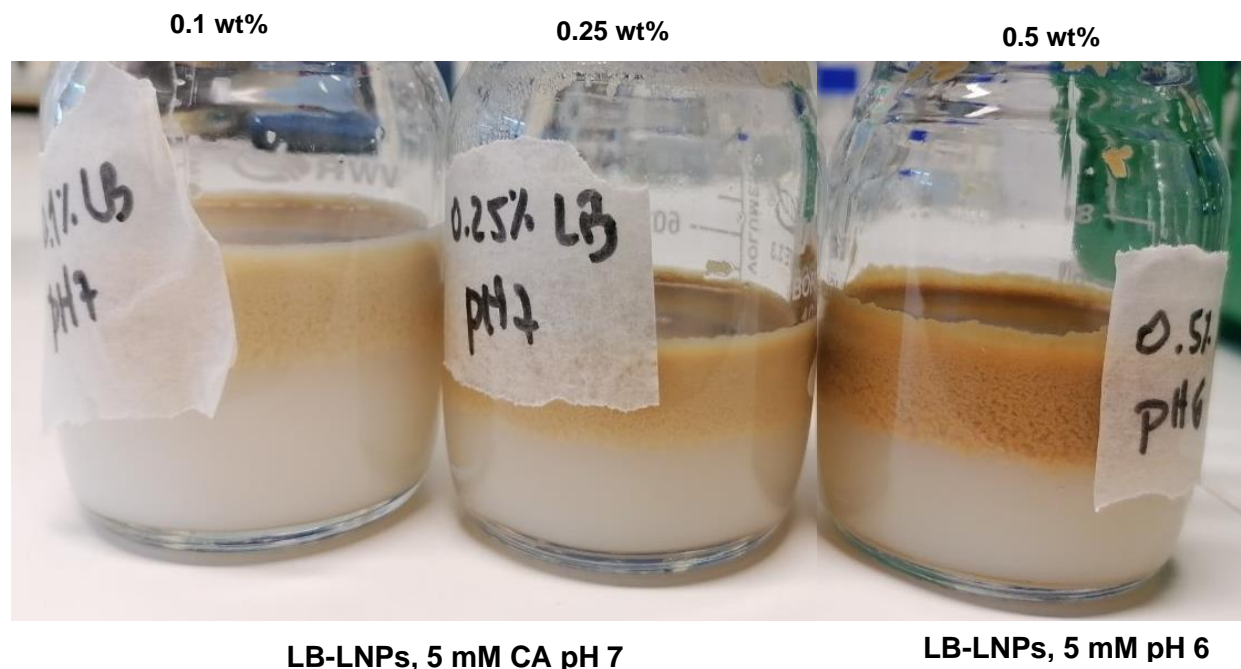


Figure 3.10 Representative pictures of the physical appearance of LB-LNPs-based emulsions, containing 5% RO, prepared in 5 mM CA buffer at pH 7 (0.1 and 0.25 w/w%) and pH 6 (0.5 w/w%), using microfluidizer.

1.1.3 Preparation of emulsions using ultrasonication utilizing RO and HD

An alternative to RO and another method of homogenization was carried out to obtain stable emulsions using LB-LNPs, and compared to BB- and PB-LNPs.

Ultrasonicated BB-LNPs-based emulsions showed better PSD with HD than RO, showing mainly one sharp peak at around 1 μm size, while the peaks with RO were broad in addition to another smaller peak at around 100 μm , for each LNP concentration (Figure 3.11). They exhibited appropriate emulsion appearance and spherical droplets (Figure 3.12). Such difference in PSD was not notable, and might be due to the presence of demulsified oil. Moreover, span, $D_{3,2}$, and $D_{4,3}$ parameters were calculated and listed in Table 3.4.

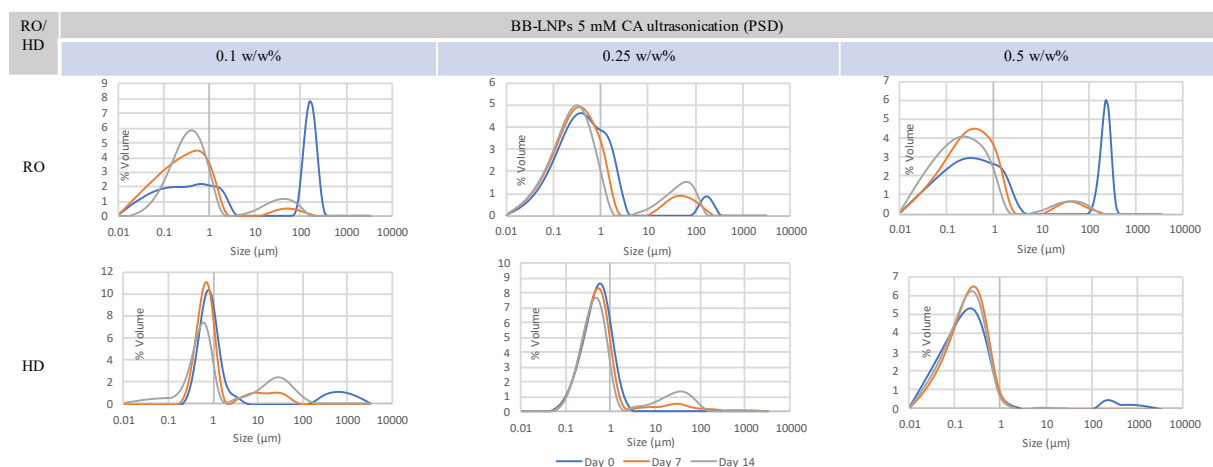


Figure 3.11 PSD plots of 0.1, 0.25 and 0.5 w/w% BB-LNPs-based emulsions, containing 5% RO or HD, prepared in 5 mM CA buffer at pH 7 using ultrasonication, at day 0, 7, and 14.

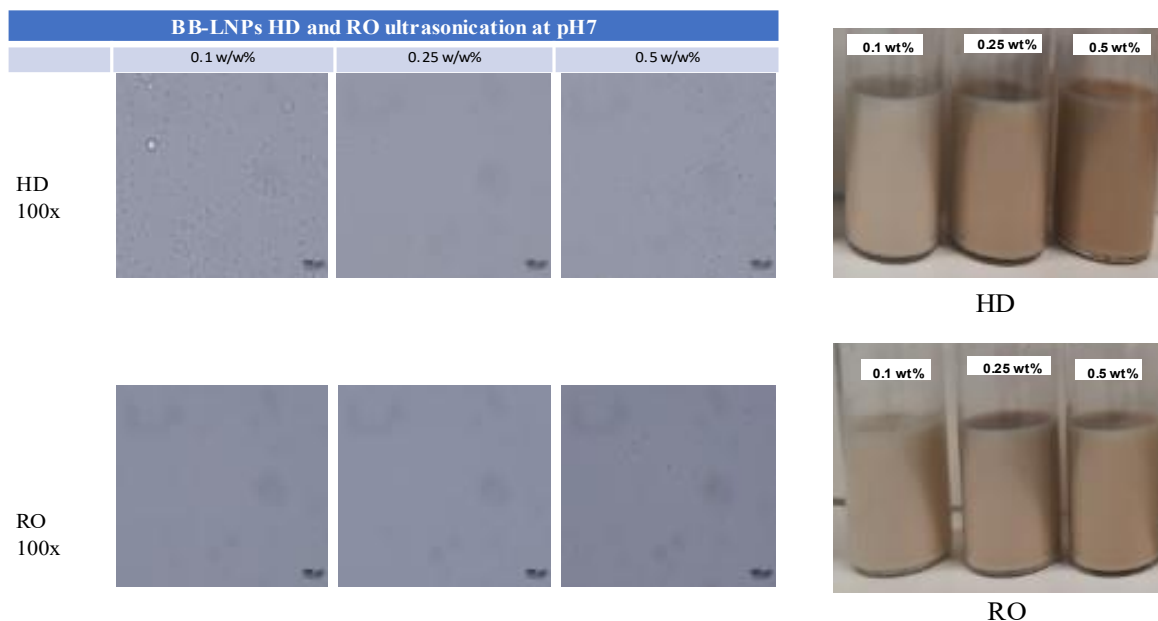


Figure 3.12 Representative pictures of the physical appearance and optical microscopy (100x magnification) of 0.1, 0.25 and 0.5 w/w% BB-LNPs-based emulsions, containing 5% RO or HD, prepared in 5 mM CA buffer at pH 7 using ultrasonication, at the day of preparation.

Table 3.4 Span, $D_{3,2}$, and $D_{4,3}$ parameters' mean \pm SD values are listed for BB-LNPs 5 mM CA ultrasonication at different conditions of oil and concentration. Statistical analysis was carried out by one-way ANOVA where unshared letters between each parameter' column is the significance value at $p \leq 0.05$.

Samples	BB-LNPs 5 mM CA ultrasonication pH 7		
	Span	$D_{3,2}$ (μm)	$D_{4,3}$ (μm)
0.1 w/w% RO	2902.312 \pm 2138.547 ^a	0.3192 \pm 0.316643 ^b	66.63333 \pm 32.24629 ^a
0.25 w/w% RO	568.3331 \pm 955.9993 ^a	0.192667 \pm 0.018502 ^b	9.071333 \pm 14.57405 ^a
0.5 w/w% RO	4107.334 \pm 1395.23 ^a	0.165 \pm 0.061213 ^b	56.1 \pm 24.71012 ^a
0.1 w/w% HD	828.4367 \pm 1431.66 ^a	0.951333 \pm 0.379896 ^a	140.3163 \pm 241.3471 ^a
0.25 w/w% HD	3.625705 \pm 0.013182 ^a	0.372 \pm 0.001 ^b	0.613 \pm 0 ^a
0.5 w/w% HD	1920.403 \pm 3301.067 ^a	0.0897 \pm 0.005977 ^b	35.21567 \pm 49.5353 ^a

Ultrasonicated PB-LNPs-based emulsions experienced almost a monomodal system with a main single peak at around 1 μm for each emulsion and physically uniform. However, the emulsions prepared with 0.1 and 0.5 w/w% PB-LNPs and 5% HD exhibited a second peak ranging from 1 to 40 μm . (Figure 3.13 and Figure 3.14)

Regarding the PSD of LB-LNPs-based emulsions, the peaks were not uniform but rather broad and extended up to 100 μm , in case of the presence of one peak (Figure 3.15). When two peaks were present, they were located at around 1 and 100 μm . This was reflected in the physical appearance of the emulsions, in which a small layer containing some LNPs was present at the top of the emulsion (Figure 3.15 and Figure 3.16).

Observing the physical appearance of LB-LNPs based HD and RO emulsions after preparation, HD-based ones showed uniform preparation, while RO-based ones showed aggregated LNPs' layer at the top of the vial. Thus, LB-LNPs-based HD emulsions were better emulsions than in HD indicating that RO impacted the produced emulsions. (Figure 3.16). Moreover, span, $D_{3,2}$, and $D_{4,3}$ parameters for PB and LB-LNPs based emulsions were calculated and listed in Table 3.5 and Table 3.6.

Overall, LB-LNPs-based emulsion looked better with ultrasonication than with microfluidizer approach of emulsification (Figure 3.10). This might suggest that the ultrasonication homogenized emulsion components without a strong impact on the LNP aggregation and phase separation of the emulsion, owing the different physical forces of shearing, cavitation, elongation, and turbulent flows employed in the two devices of emulsification that can impact the droplet formation/disruption.[64]

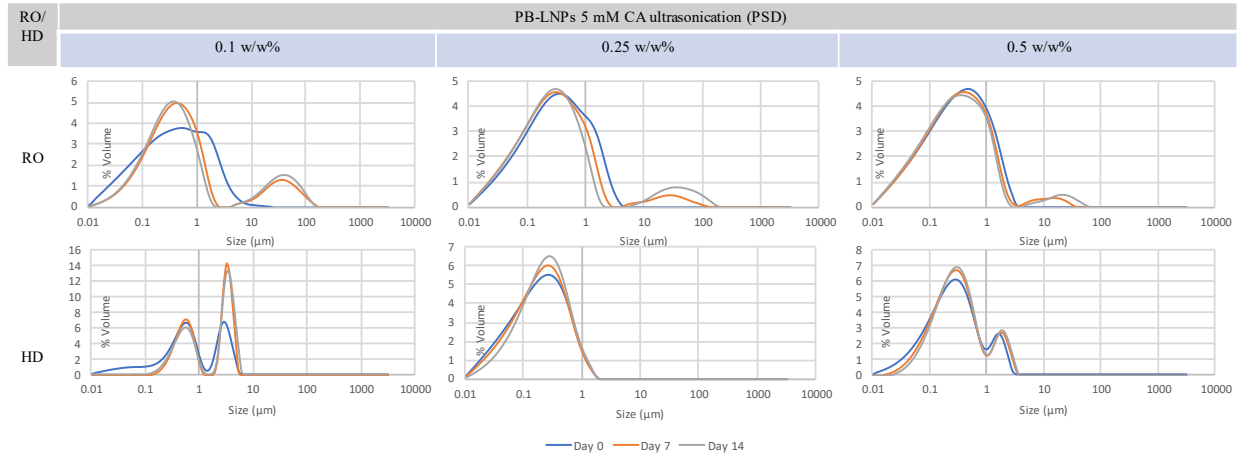


Figure 3.13 PSD plots of 0.1, 0.25 and 0.5 w/w% PB-LNPs-based emulsions, containing 5% RO or HD, prepared in 5 mM CA buffer at pH 7 using ultrasonication, at day 0, 7, and 14.

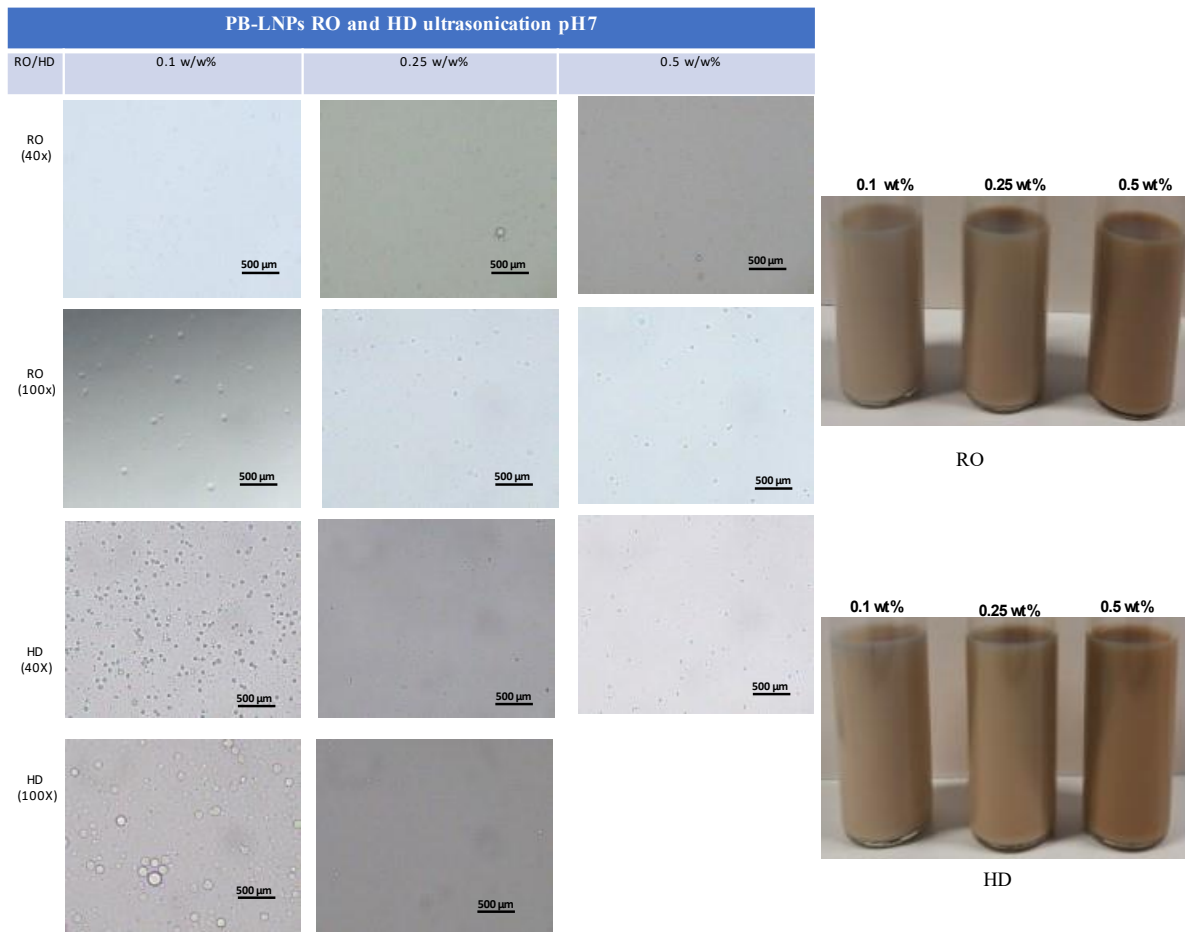


Figure 3.14 Physical and microscopical characterization (with 40x and 100x magnifications) at 0 day of 0.1, 0.25 and 0.5 w/w% PB LNPs forming 5% RO and HD emulsions at pH 7.

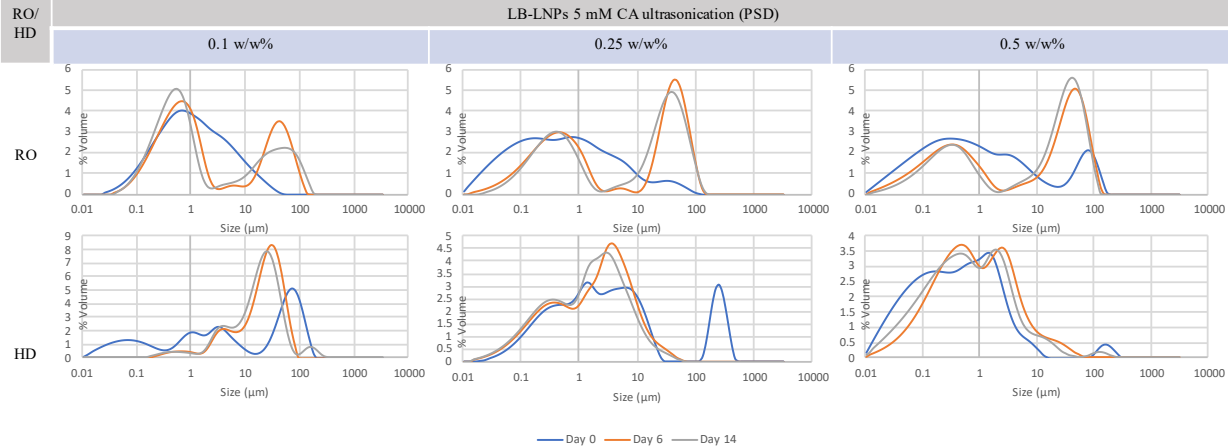


Figure 3.15 PSD plots of 0.1, 0.25 and 0.5 w/w% LB-LNPs-based emulsions, containing 5% RO or HD, prepared in 5 mM CA buffer at pH 7 using ultrasonication, at day 0, 6, and 14.

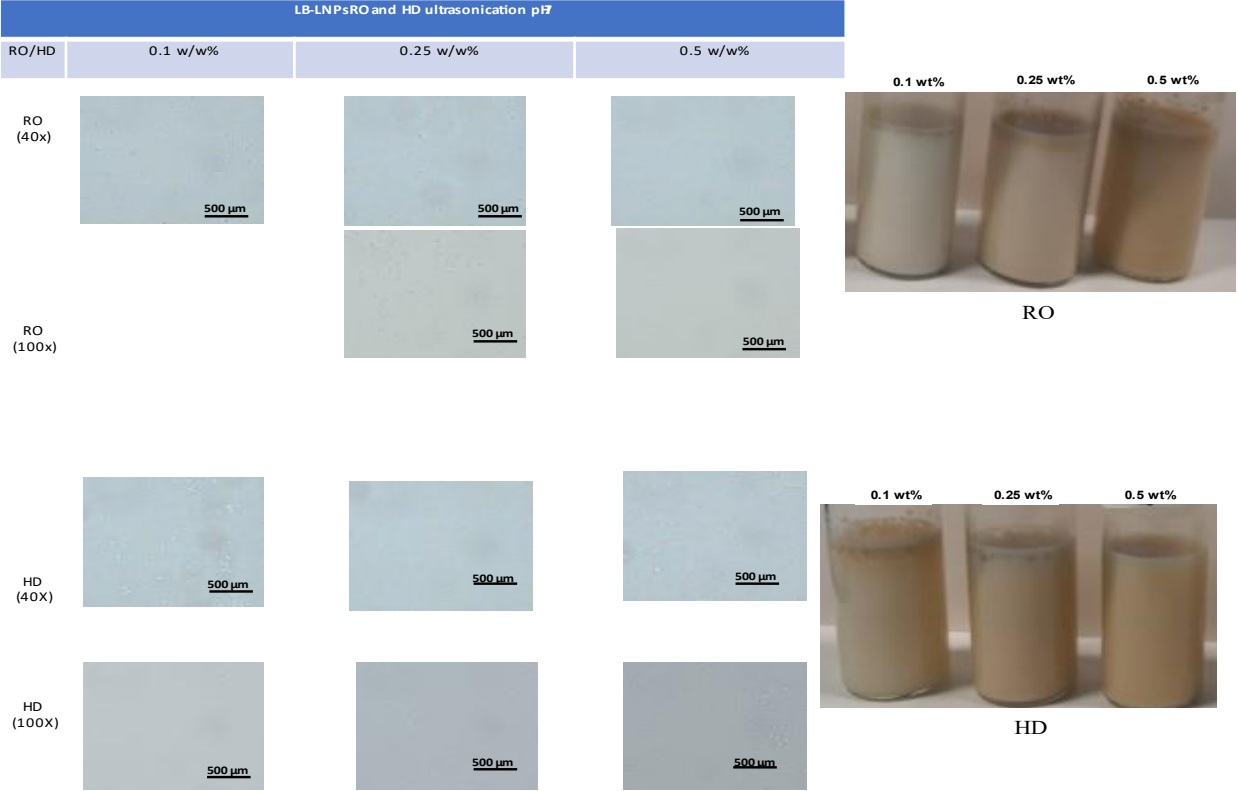


Figure 3.16 Physical and microscopical characterization (with 40x and 100x magnifications) at 0 day of 0.1, 0.25 and 0.5 w/w% LB LNPs forming 5% RO and HD emulsions at pH 7 with ultrasonication.

Table 3.5 Span, $D_{3,2}$, and $D_{4,3}$ parameters' mean \pm SD values are listed for PB-LNPs 5 mM CA ultrasonication at different conditions of oil and concentration. Statistical analysis was carried out by one-way ANOVA where unshared letters between each parameter' column is the significance value at $p \leq 0.05$.

Samples	PB-LNPs 5 mM CA ultrasonication pH 7		
	Span	$D_{3,2}$ (μm)	$D_{4,3}$ (μm)
0.1 w/w% RO	31.20602 ± 21.61043^a	0.183867 ± 0.093767^a	$0.892667 \pm 0.256946^{ab}$
0.25 w/w% RO	21.95313 ± 0.127858^a	0.135 ± 0^a	0.57 ± 0.003606^{bc}
0.5 w/w% RO	19.81323 ± 0.022909^a	0.13 ± 0^a	$0.522667 \pm 0.000577^{bc}$
0.1 w/w% HD	34.41601 ± 43.62116^a	0.4619 ± 0.315413^a	1.314667 ± 0.330008^a
0.25 w/w% HD	11.92876 ± 0.002905^a	0.096533 ± 0.000115^a	0.281 ± 0^c
0.5 w/w% HD	16.10407 ± 0.051689^a	0.148 ± 0^a	0.464 ± 0.001^{bc}

Table 3.6 Span, $D_{3,2}$, and $D_{4,3}$ parameters' mean \pm SD values are listed for LB-LNPs 5 mM CA ultrasonication at different conditions of oil and concentration. Statistical analysis was carried out by one-way ANOVA where unshared letters between each parameter' column is the significance value at $p \leq 0.05$.

Samples	LB-LNPs 5 mM CA ultrasonication pH 7		
	Span	$D_{3,2}$ (μm)	$D_{4,3}$ (μm)
0.1 w/w% RO	41.62486 ± 2.384702^a	0.411333 ± 0.010693^a	2.88 ± 0.20664^a
0.25 w/w% RO	135.7635 ± 38.42665^a	0.166433 ± 0.081052^a	3.863333 ± 1.425494^a
0.5 w/w% RO	1048.398 ± 187.6481^a	0.167 ± 0.00755^a	13.7 ± 2.882707^a
0.1 w/w% HD	1039.711 ± 1523.456^a	0.516167 ± 0.380955^a	31.9 ± 10.39375^a
0.25 w/w% HD	793.9183 ± 646.0431^a	0.561333 ± 0.108611^a	41.93 ± 36.17217^a
0.5 w/w% HD	56.05881 ± 18.85646	0.1464 ± 0.066416^a	4.988667 ± 7.028618^a

Following the stability profile over 14 days of the three types of LNPs-based emulsions prepared with ultrasonication, the second peak on the PSD of BB-LNPs-based emulsions that appeared at day 0 diminished (Figure 3.11). In addition, these emulsions were stable over the 14 days duration, exhibiting PSD values almost consistent during the storage period, with exception of the LB-LNPs-based emulsions with 5% RO, which exhibited large droplet sizes around 100 μm . Regarding the TSI values, the results presented higher values for HD than for RO emulsions, and they almost decreased with concentration increase (Figure 3.17, Figure 3.18 and Figure 3.19). All prepared emulsions experienced creaming where larger particles floated to the top of the emulsions during storage. This complies with the concept that after the period of storage, creaming and flocculation can occur, and large or flocculated droplets move upwards into the top of the emulsion, leading to backscattering decrease at the bottom and increase at the top of the containing vial.[92] This was reflected in the increasing TSI values over time. RO or HD and the interactions between ingredients

can effect of the emulsion stability by impacting the particle size of the droplets and disturbing concentration of the stabilizers [63]

Comparing the homogenization methods here employed for the emulsion preparation, BB- and PB-LNPs-based emulsions obtained using microfluidizer exhibited better results, while ultrasonication was found to be a better technique for preparing LB-LNPs-based emulsions. Overall, most formulations were considered emulsified samples when the droplet size ranged between 1 to 100 μm . [63]

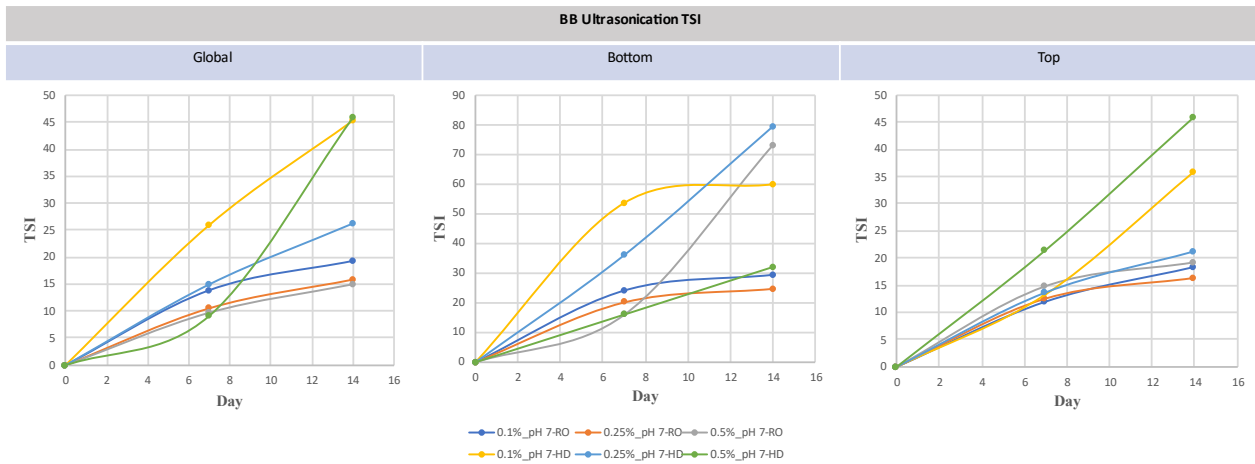


Figure 3.17. Global, bottom, and top TSI values for 0.1, 0.25 and 0.5 w/w% BB-LNPs-based emulsions, containing 5% RO or HD, prepared in 5 mM CA buffer at pH 7 using ultrasonication, over 14 days.

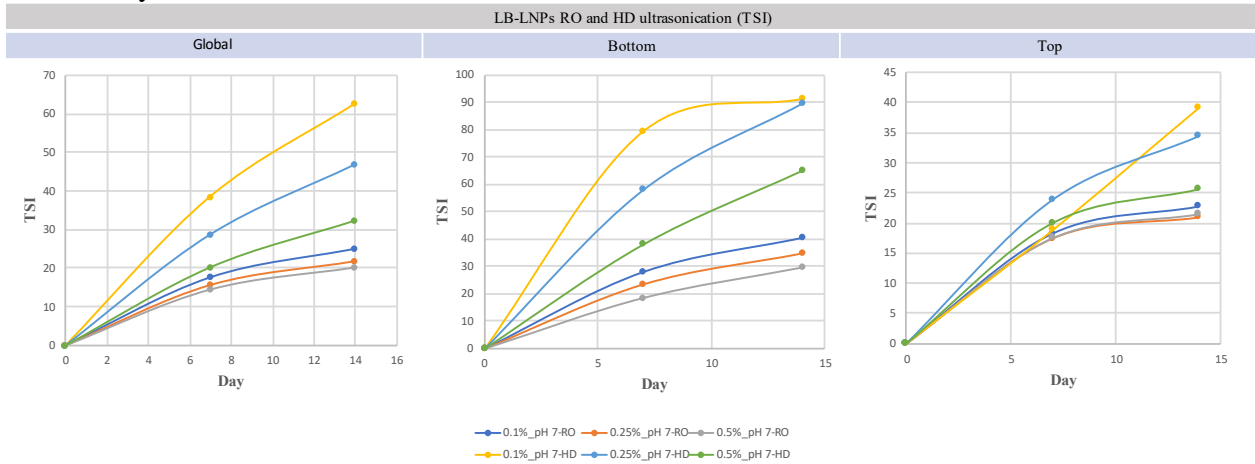


Figure 3.18 Global, bottom, and top TSI stability indicators for various ultrasonicated 5% RO and HD emulsions using 0.1, 0.25 and 0.5 w/w% LB LNPs of pH 7 at 0, 7 and 14 days intervals.

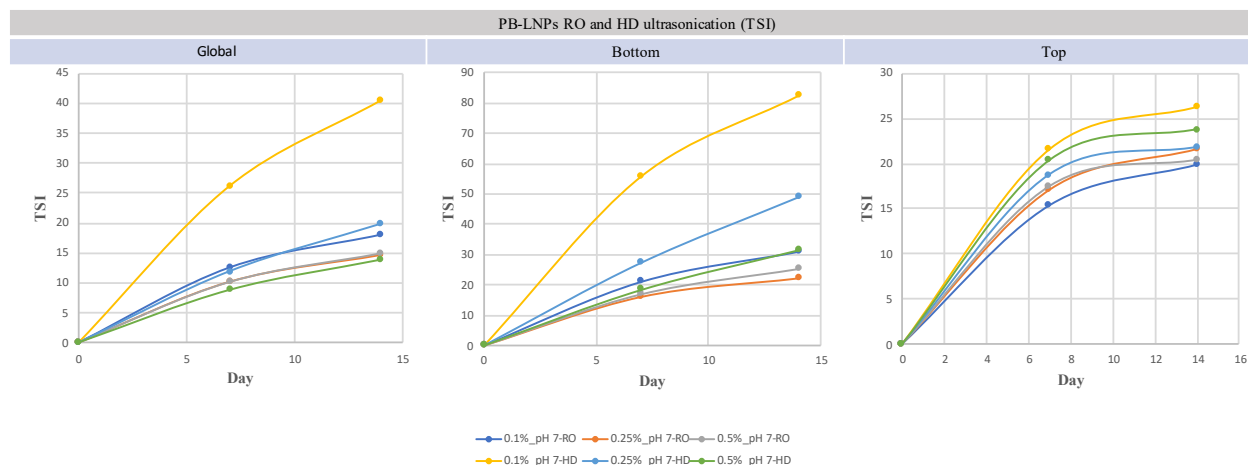


Figure 3.19 Global, bottom, and top TSI stability indicators for various ultrasonicated 5% RO and HD emulsions using 0.1, 0.25 and 0.5 w/w% PB LNPs of pH 7 at 0, 7- and 14-days intervals.

1.2 Phenolic content determination of LNPs-based emulsions

In addition to the emulsifying properties of LNPs, the phenolic content of LNPs-based emulsions was also evaluated. After conducting the spectrophotometric method based on the Folin-Ciocalteu reagent required to determine free phenolic groups, the results varied according to the concentration of LNPs, and also with the type of oil (RO and HD) used in the preparation of emulsions (Figure 3.20).

The phenolic content determined as mmol Van eq/l of lignin were found to be concentration dependent, where increased LNP concentration in the emulsions led to an increase in the phenolic content (mmol Van eq/l of lignin). To investigate the effect of utilizing RO and HD on the phenolic content, the all the emulsions prepared with 5% RO showed higher phenolic content than the ones prepared with 5% HD. This can be rationalized by the higher attachment of LNPs at the O/W interface and consequently, less availability for free phenolic groups to be determined. Moreover, LB-LNPs-based emulsions exhibited the lowest phenolic content than the PB- and BB-LNPs-based emulsions caused by the difference in each lignin constituting units.

Calculation of the phenolic content in terms of mmol Van eq/g of lignin, where the values were normalized by the amount of lignin in each sample, different patterns on results were observed for both RO and HD emulsions. The phenolic content (mmol Van eq/g of lignin) in HD based preparations were concentration dependent, as increasing the concentration of LNPs led to an increased phenolic content. However, for HD-based emulsions containing 0.5 w/w% BB- and PB-LNPs experienced almost similar increase as at LNP concentration of 0.25 w/w% of about 1 mmol Van eq/g of lignin. Generally, RO-based emulsions presented higher phenolic content than the HD-based ones at lower LNP concentrations of 0.1 and 0.25 w/w%. In RO samples, the phenolic content was inversely proportional to the concentration of BB-LNPs in the emulsions. While this relation was not observed in case of LB and PB-LNPs based samples. Likewise, that can be explained by the possible increased attachment interactions of the free phenolic functional groups as the concentration of the sample increased in presence of RO. PB based samples experienced less interactions of their LNPs' free phenolic groups compared to other two types of emulsions. However, the case is not the same in presence of HD. At 0.1 w/w% of LNPs concentration, BB-LNPs showed the highest phenolic content, whereas at 0.25 and 0.5 w/w% exhibited highest

phenolic content for PB-LNPs based emulsions. Moreover, the phenolic content for BB, PB and LB-LNPs based emulsions were ANOVA processed and listed in Table 3.7 and Table 3.8

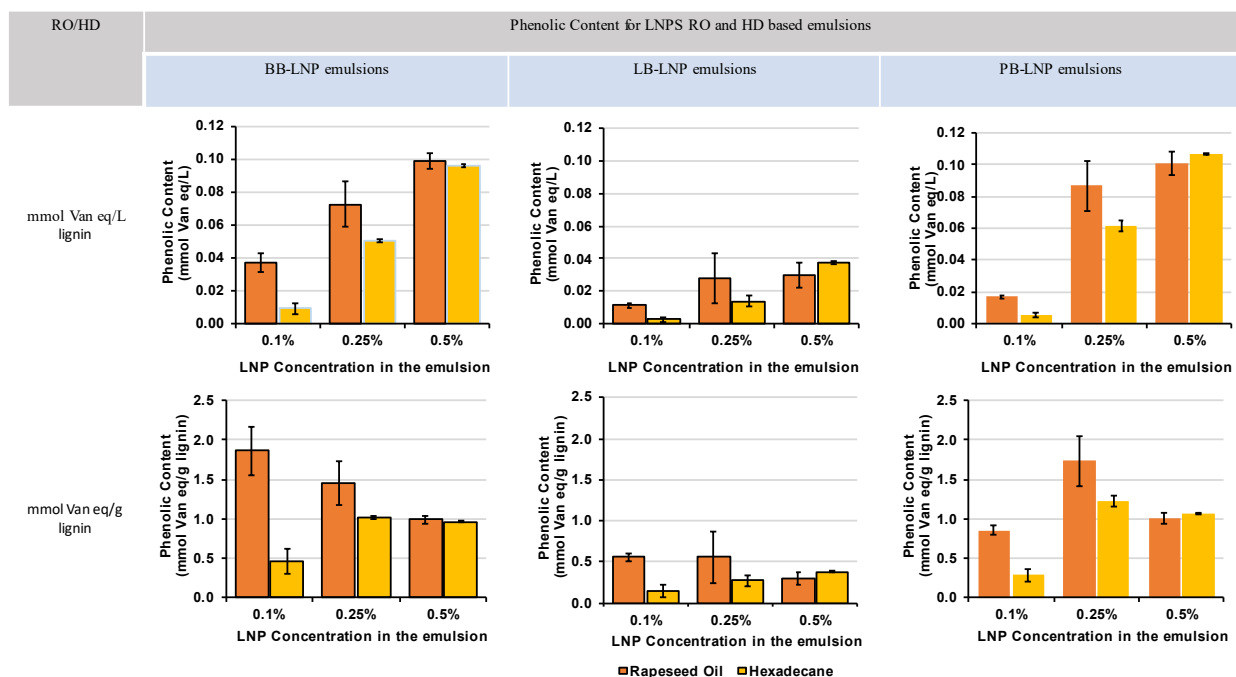


Figure 3.20 Phenolic content of 0.1, 0.25 and 0.5 w/w% LNPs-based emulsions (in three replicates), containing 5% RO or HD, prepared in 5 mM CA buffer at pH 7 using ultrasonication, at day 0.

Table 3.7 Phenolic content of RO and HD for BB, PB and LB-LNPs-based emulsions expressed as mmol Van eq/g lignin (mean \pm SD) for different concentrations. Statistical analysis was carried out by one-way ANOVA where unshared letters between each LNPs' group is the significance value at $p \leq 0.05$.

5 mM CA ultrasonicated pH 7 samples	mmol Van eq/g lignin (mean \pm SD)		
	BB-LNPs	PB-LNPs	LB-LNPs
0.1 w/w% RO	0.037258 \pm 0.006039 ^c	0.017068 \pm 0.002039 ^e	0.010408 \pm 0.001438 ^{bc}
0.25 w/w% RO	0.072592 \pm 0.013761 ^b	0.086681 \pm 0.000559 ^c	0.027962 \pm 0.015781 ^{ab}
0.5 w/w% RO	0.099101 \pm 0.004739 ^a	0.10059 \pm 0.002478 ^b	0.029632 \pm 0.007454 ^{ab}
0.1 w/w% HD	0.009042 \pm 0.003159 ^d	0.005629 \pm 0.003637 ^f	0.00276 \pm 0.001463 ^c
0.25 w/w% HD	0.050622 \pm 0.000989 ^c	0.061588 \pm 0.001557 ^d	0.013654 \pm 0.003524 ^{bc}
0.5 w/w% HD	0.096522 \pm 0.001039 ^a	0.106581 \pm 0.000742 ^a	0.037549 \pm 0.000725 ^a

Table 3.8 Phenolic content of RO and HD for BB, PB and LB-LNPs-based emulsions expressed as mmol Van eq/L lignin (mean \pm SD) for different concentrations. Statistical analysis was carried out by one-way ANOVA where unshared letters between each LNPs' group is the significance value at $p \leq 0.05$.

5 mM CA ultrasonicated pH 7 samples	mmol Van eq/L lignin (mean \pm SD)		
	BB-LNPs	PB-LNPs	LB-LNPs
0.1 w/w% RO	0.037258 \pm 0.006039 ^c	0.017068 \pm 0.002039 ^e	0.010656 \pm 0.001099 ^{bc}
0.25 w/w% RO	0.072592 \pm 0.013761 ^b	0.086681 \pm 0.000559 ^c	0.027962 \pm 0.015781 ^{ab}
0.5 w/w% RO	0.099101 \pm 0.004739 ^a	0.10059 \pm 0.002478 ^b	0.029632 \pm 0.007454 ^{ab}
0.1 w/w% HD	0.009042 \pm 0.003159 ^d	0.005629 \pm 0.003637 ^f	0.00276 \pm 0.001463 ^c
0.25 w/w% HD	0.050622 \pm 0.000989 ^c	0.061588 \pm 0.001557 ^d	0.013654 \pm 0.003524 ^{bc}
0.5 w/w% HD	0.096522 \pm 0.001039 ^a	0.106581 \pm 0.000742 ^a	0.037549 \pm 0.000725 ^a

1.3 Antioxidant activity of LNPs

The three different LNPs were assessed for their antioxidant activity using the DPPH assay (Figure 3.21). The DPPH inhibition ability of LNPs expressed as mg AA eq/g of lignin were ranging between 230 and 500. The values decreased as the LNP concentration increased. Similarly, owing to the direct relation between phenolic content and antioxidant, the results led to the previous findings with phenolic content where the higher the sample concentration of LNPs the less phenolic content and antioxidant activity per g of LNPs.

Analyzing the DPPH inhibition percentage of the total amount of LNPs, the results showed that the higher the concentration of LNPs, the higher the inhibition and the antioxidant activity. This is due to the higher amount of the total phenolic groups when the concentration of LNPs in the samples is higher. Although the variance between the three different LNPs values was not high, BB-LNPs showed relatively higher effectiveness than the other two types of LNPs, and LB-LNPs showed the lowest DPPH inhibition. Such variance in the antioxidant activity among the three LNPs can be attributed to the difference in lignin units in each type of lignin (S vs G). Moreover, the antioxidant activity for BB, PB and LB-LNPs suspensions were ANOVA processed and listed in Table 3.9 and Table 3.10.

The suggested mechanism by which antioxidant initiated is single electron transfer and hydrogen transfer reactions, which is impacted by the available number of -OH and -OCH₃ functional groups. Lignin limitation to be employed on the chemical industry is the inhomogeneity and with nanoparticles preparation this limitation can be eliminated providing the path to be utilized in chemical and pharmaceutical industries as antioxidant natural agent. [93-95]

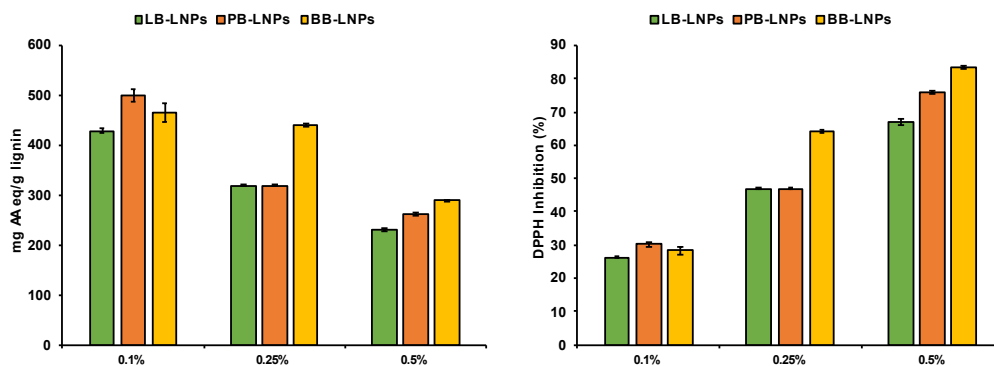


Figure 3.21 Antioxidant activity expressed in DPPH inhibition and mg AA eq/g lignin of 0.1, 0.25 and 0.5 w/w% LNP suspensions.

Table 3.9 Antioxidant activity for BB, PB and LB-LNPs-based emulsions expressed as mg AA eq/g lignin (mean \pm SD) for different concentrations. Statistical analysis was carried out by one-way ANOVA where unshared letters between each LNPs' group is the significance value at $p \leq 0.05$.

Sample	mg AA eq/g lignin (mean \pm SD)		
	BB-LNPs	PB-LNPs	LB-LNPs
LNPs 0.1 w/w%	465.9670757 \pm 17.98285419 ^a	499.8859147 \pm 11.79881 ^a	428.9807325 \pm 4.875267987 ^a
LNPs 0.25 w/w%	440.7428642 \pm 3.210669137 ^a	318.733768 \pm 2.05369 ^b	318.6068368 \pm 1.539540596 ^b
LNPs 0.5 w/w%	288.7450419 \pm 1.335349627 ^b	261.9414022 \pm 1.944246 ^c	230.596446 \pm 2.774478607 ^c

Table 3.10 Antioxidant activity for BB, PB and LB-LNPs-based emulsions expressed as DPPH inhibition % (mean \pm SD) for different concentrations. Statistical analysis was carried out by one-way ANOVA where unshared letters between each LNPs' group is the significance value at $p \leq 0.05$.

samples	DPPH inhibition (%) (mean \pm SD)		
	BB-LNPs	PB-LNPs	LB-LNPs
LNPs 0.1 w/w%	28.25490274 \pm 1.014413 ^c	30.16826 \pm 0.665571 ^c	26.16850312 \pm 0.275014 ^c
LNPs 0.25 w/w%	64.12546243 \pm 0.452785 ^b	46.91913 \pm 0.289622 ^b	46.90122917 \pm 0.217114 ^b
LNPs 0.5 w/w%	83.41023907 \pm 0.376635 ^a	75.85027 \pm 0.548375 ^a	67.00942758 \pm 0.782542 ^a

1.4 Antibacterial inhibition of LNPs

As one of the study purposes, LNP suspensions were tested for their antibacterial activity. Upon incubation of 0.5 w/w% LNPs at pH 6 against *Staphylococcus aureus* and *E. coli* in the screening experiment, the three types of LNPs showed strong activity to inhibit the growth of *Staphylococcus aureus* (complete inhibition at 10^{-3} , 10^{-4} and 10^{-5} dilution levels and few colonies of growth at 10^{-1} and 10^{-2} compared to the control), while slight inhibition against *E. coli* was observed, BB-LNPs showed the highest activity followed by PB- and LB-LNPs after 4 h contact time. Results were compared to the control results and described qualitatively (Figure 3.22, Figure 3.23 and Table 3.11). Investigating quantitatively the magnitude of the inhibition activity of BB-LNPs against *Staphylococcus aureus*, BB-LNPs achieved around 3 log reductions of *Staphylococcus aureus* according to the below equation (Figure 3.24 and Table 3.12).

$$\text{Log reduction} = \text{Log} \frac{\text{control}}{\text{sample}} = \log \frac{3060}{4} = 2.88 \text{ log reductions}$$

Such clear difference in the antibacterial response against the two types of bacteria can be justified based on the difference in cellular barriers presented in presence of thicker lipopolysaccharide layer in gram-positive *Staphylococcus aureus* while a thinner layer in gram-negative bacteria (*E. coli*) that might affect differently the contact of LNPs to the cellular structure of the bacteria leading different responses. Also, the variable activity of the individual LNPs on each bacterium can be justified by the difference in the variable content of antibacterial structures of each LNPs, the different source and the extraction or preparation processes employed to produce these particles

[77]. This falls in accordance with previous reports on lignin composites, where lignin exhibited antibacterial functionality against *S. aureus* while no effect on gram negative *E. coli* [96, 97].

There are two mechanisms suggested by which lignin phenolic domain possesses its antibacterial activity suppressing growth of microorganisms, the physiological reactive oxygen species redox and Trojan horse mechanisms. In the Trojan horse mechanism, LNPs suggested to break into the bacterial cell difficultly through its membrane [86].

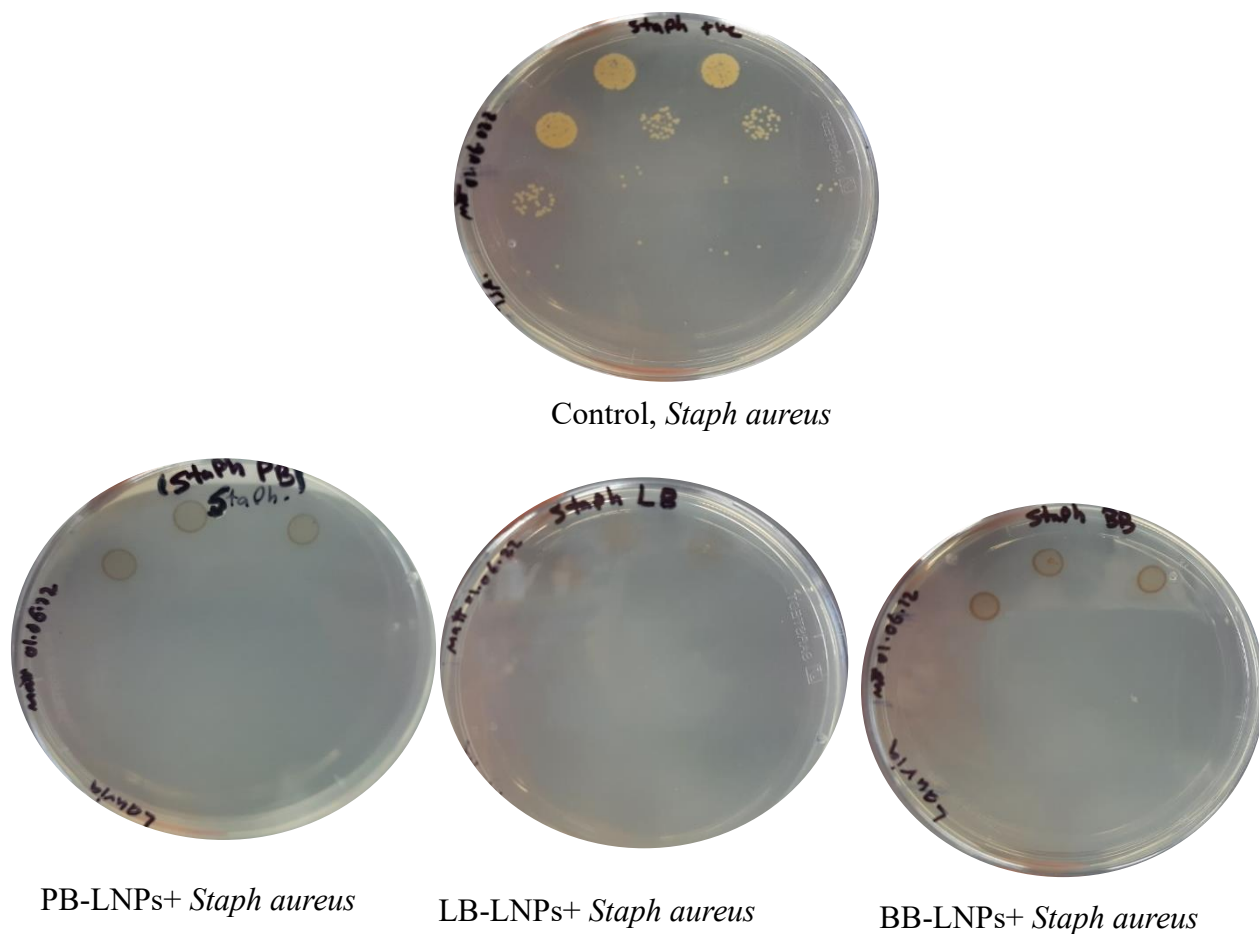


Figure 3.22 Screening of bacterial inhibition of 0.5 w/w% of LB-, BB- and PB-LNPs at pH 6 against *Staphylococcus aureus* after 4 h contact compared with the control.

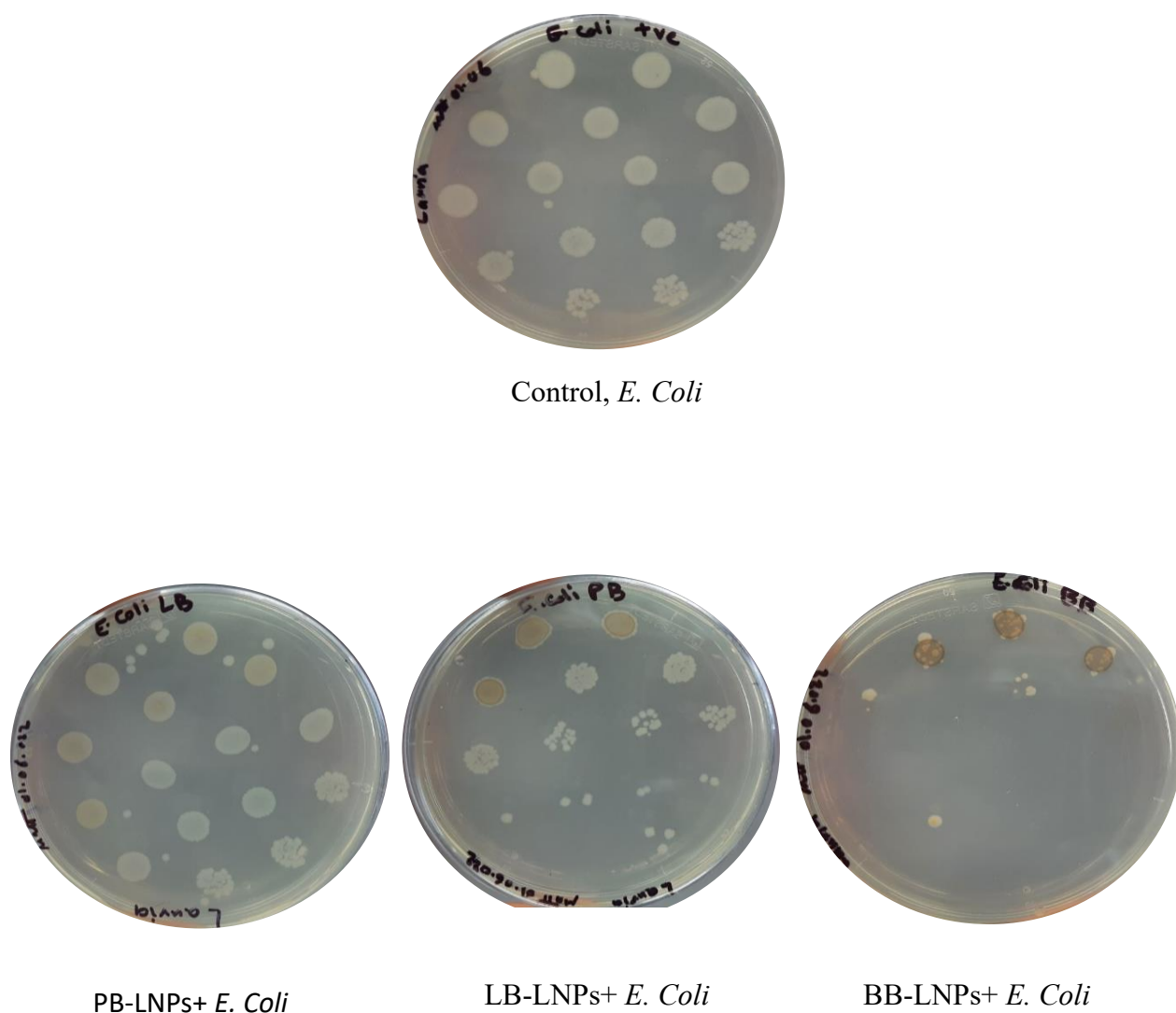


Figure 3.23 Screening of the bacterial inhibition after incubation of 0.5 w/w% of LB-, BB- and PB-LNPs at pH 6 against *E. coli* after 4 h contact compared with the control.

Table 3.11 Qualitative bacterial inhibition of 0.5 w/w% of LB-, BB- and PB-LNPs at pH 6 against *Staphylococcus aureus* and *E. coli* after 4 h contact compared with the control. LNPs inhibition results were compared relatively to the control.

Test	Replicate	<i>E. coli</i> (CFUs)					<i>Staph aureus</i> (CFUs)				
		10 ⁻¹	10 ⁻²	10 ⁻³	10 ⁻⁴	10 ⁻⁵	10 ⁻¹	10 ⁻²	10 ⁻³	10 ⁻⁴	10 ⁻⁵
Control	C1	OG	OG	OG	OG	LOG	OG	58	12	NG	NG
	C2	OG	OG	OG	OG	LOG	OG	51	16	NG	NG
	C3	OG	OG	OG	OG	LOG	OG	54	11	NG	NG
LB-LNPs	R1	S	RL	RL	RL	L	L	L	27	3	NG
	R2	S	RL	RL	RL	L	L	L	34	3	NG
	R3	S	RL	RL	RL	L	L	L	20	5	NG
	R1	S	RL	L	L	L	1	3	NG	NG	NG

BB-LNPs	R2	S	RL	L	L	L	4	2	NG	NG	NG
	R3	S	RL	L	L	L	1	2	NG	NG	NG
PB-LNPs	R1	S	RL	RL	L	L	13	5	NG	NG	NG
	R2	S	RL	RL	L	L	16	3	NG	NG	NG
	R3	S	RL	RL	L	L	13	9	NG	NG	NG

Abbreviations: C: control, R: replicate, OG: overgrowth, LOG: less overgrowth, NG: no growth, S: similar to control, RL: relatively less than control, L: less than control



0.1ml *Staph aureus* (10^{-1}) control
HTBC= 3060 CFUs



0.1ml *Staph aureus* (10^{-2}) control
306 CFUs



0.1ml (LNPs+ *Staph aureus*) (10^{-1})
4 CFUs



0.1ml (LNPs+ *Staph aureus*) (10^{-1})
(NG)

Figure 3.24 Comparison of the grown colonies of 0.1 mL *Staphylococcus aureus* strains control (10^{-1} and 10^{-2}) and the counted colonies after 4 h contact inhibition of 0.1 mL 0.5 w/w% of BB-LNPs (10^{-1} and 10^{-2}) at pH 6 against *Staphylococcus aureus*. Abbreviations: NG: no growth, CFUs: colony forming units, HTBC: high to be count.

Table 3.12. Quantitative results of bacterial inhibition of 0.5 w/w% of BB-LNPs at pH 6 against *Staphylococcus aureus* after 4 h contact compared with the control.

BB-LNPs after 4 h contact and control with surface spread technique						
Dilution level		10 ⁻¹	10 ⁻²	10 ⁻³	10 ⁻⁴	10 ⁻⁵
Sample	0.1 ml <i>Staph aureus</i> + BB-LNPs (CFUs)	4	NG	NG	NG	NG
Control	0.1 ml <i>Staph aureus</i> (CFUs)	HTBC Around 3060	306	47	13	NG

Abbreviations: CFUs: colony forming units, NG: no growth, HTBC: high to be count

Chapter 4: Conclusions and future directions

This comparative study evaluated LNPs from different sources' (BB-, PB and LB-LNPs) activities (emulsifying, antioxidant, and antibacterial functions) at three concentrations (0.1, 0.25 and 0.5 w/w% LNPs). The study not only compared these activities, but further assessed the incorporating different variables for these functions. In emulsifying part, several factors were assessed including: effect of ionic strength and pH, LNPs' concentration in stabilizing emulsion, oil type involved in the o/w emulsions, and emulsifying technique. In the antibacterial section, both gram-positive and gram-negative bacteria were employed to challenge LNPs' inhibitory power at 4 h contact time and with number of log reductions achieved against *Staphylococcus aureus*. Also, LNPs prepared from the three lignin sources were assessed for their DPPH inhibitory percentage, while their corresponding based emulsions with RO and HD were evaluated for their total phenolic content.

These tests' results concluded that 5 mM CA ionic strength at pH 7 was the most optimum variable among others to obtain uniform emulsion. For the homogenizing approach, microfluidization favored BB- and PB-LNPs based emulsions over LB-LNPs, while ultrasonication showed the opposite. Generally, LNPs' concentration increase was accompanied with higher stability. The oil choice in o/w preparations impacted the results to less extent. RO-Based preparation presented a slightly higher optimizing condition for PB-LNPs stabilizers and for higher phenolic content compared to HD ones. On the other hand, HD-based samples favored LB-LNPs and BB-LNPs to exhibit slightly higher emulsifying effect compared to the two LNPs.

The three LNPs varied in their emulsifying capacity, PB-LNPs showed the highest effect close to the BB-LNPs effect, while LB-LNPs showed the lowest. LNPs at 0.5 w/w% showed strong inhibition against two types of bacteria. While LNPs showed bactericidal effect on *Staphylococcus aureus* and achieved roughly 3 reduction logs, the inhibition in case of *E. coli* was at 1 log. Both BB- and PB-based samples showed higher total phenolics and in correlation with antioxidant activity than LB-LNPs.

This study can be the basis to test more variables such as different homogenization parameters or techniques, antifungal activity, different bacterial contact times at less than 4 h in the future. The addition of another stabilizer, incorporating LNPs in food emulsions and packaging should be the next logical step to capitalize on their food and drugs applications. >>→

Chapter 5: References

1. Tuck, C.O., et al., *Valorization of biomass: deriving more value from waste*. Science, 2012. **337**(6095): p. 695-9.
2. Kai, D., et al., *Towards lignin-based functional materials in a sustainable world*. Green Chemistry, 2016. **18**(5): p. 1175-1200.
3. Boerjan, W., J. Ralph, and M. Baucher, *Lignin biosynthesis*. Annu Rev Plant Biol, 2003. **54**: p. 519-46.
4. Erdtman, H., *Lignins: Occurrence, formation, structure and reactions*, K. V. Sarkanen and C. H. Ludwig, Eds., John Wiley & Sons, Inc., New York, 1971. 916 pp. \$35.00. 1972. **10**(3): p. 228-230.
5. Jones, L., A.R. Ennos, and S.R. Turner, *Cloning and characterization of irregular xylem4 (irx4): a severely lignin-deficient mutant of Arabidopsis*. Plant J, 2001. **26**(2): p. 205-16.
6. Dorrestijn, E., et al., *The occurrence and reactivity of phenoxyl linkages in lignin and low rank coal*. 2000. **54**: p. 153-192.
7. Upton, B.M. and A.M. Kasko, *Strategies for the Conversion of Lignin to High-Value Polymeric Materials: Review and Perspective*. Chemical Reviews, 2016. **116**(4): p. 2275-2306.
8. Nguyen, T.E., E. Zavarin, and E.M. Barrall. *Thermal Analysis of Lignocellulosic Materials. Part II. Modified Materials*. 1981.
9. Sakakibara, A., *A structural model of softwood lignin*. Wood Science and Technology, 1980. **14**(2): p. 89-100.
10. Whetten, R. and R. Sederoff, *Lignin Biosynthesis*. Plant Cell, 1995. **7**(7): p. 1001-1013.
11. Strassberger, Z., S. Tanase, and G. Rothenberg, *The pros and cons of lignin valorisation in an integrated biorefinery*. RSC Advances, 2014. **4**(48): p. 25310-25318.
12. Lora, J., *Chapter 10 - Industrial Commercial Lignins: Sources, Properties and Applications, in Monomers, Polymers and Composites from Renewable Resources*, M.N. Belgacem and A. Gandini, Editors. 2008, Elsevier: Amsterdam. p. 225-241.
13. Thakur, V.K., et al., *Progress in Green Polymer Composites from Lignin for Multifunctional Applications: A Review*. ACS Sustainable Chemistry & Engineering, 2014. **2**(5): p. 1072-1092.
14. Wu, R., et al., *Preparation, structure, and properties of poly(ethyleneoxide)/lignin composites used for UV absorption*. 2020. **137**(16): p. 48593.
15. Gao, S., et al., *Fabrication of lignin based renewable dynamic networks and its applications as self-healing, antifungal and conductive adhesives*. Chemical Engineering Journal, 2020. **394**: p. 124896.
16. Chen, Y., et al., *High-value utilization of hydroxymethylated lignin in polyurethane adhesives*. International Journal of Biological Macromolecules, 2020. **152**: p. 775-785.
17. Zhang, Z., et al., *Kinetics of partially depolymerized lignin as co-curing agent for epoxy resin*. International Journal of Biological Macromolecules, 2020. **150**: p. 786-792.
18. Zhang, Y., et al., *Preparation and characterization of chemical grouting derived from lignin epoxy resin*. European Polymer Journal, 2019. **118**: p. 290-305.
19. Ko, H.-U., et al., *Esterified PVA-lignin resin by maleic acid applicable for natural fiber reinforced composites*. 2020. **137**(26): p. 48836.
20. Anugwom, I., et al., *Lignin as a functional additive in a biocomposite: Influence on mechanical properties of polylactic acid composites*. Industrial Crops and Products, 2019. **140**: p. 111704.
21. Liu, W.-J., H. Jiang, and H.-Q. Yu, *Thermochemical conversion of lignin to functional materials: a review and future directions*. Green Chemistry, 2015. **17**(11): p. 4888-4907.

22. Naseem, A., et al., *Lignin-derivatives based polymers, blends and composites: A review*. International Journal of Biological Macromolecules, 2016. **93**: p. 296-313.
23. Wang, W., et al., *Versatile value-added application of hyperbranched lignin derivatives: Water-resistance adhesive, UV protection coating, self-healing and skin-adhesive sensing*. Chemical Engineering Journal, 2021. **404**: p. 126358.
24. Gan, D., et al., *Plant-inspired adhesive and tough hydrogel based on Ag-Lignin nanoparticles-triggered dynamic redox catechol chemistry*. Nature Communications, 2019. **10**(1): p. 1487.
25. Duval, A. and M. Lawoko, *A review on lignin-based polymeric, micro- and nano-structured materials*. Reactive and Functional Polymers, 2014. **85**: p. 78-96.
26. Sipponen, M.H., et al., *Lignin for Nano- and Microscaled Carrier Systems: Applications, Trends, and Challenges*. ChemSusChem, 2019. **12**(10): p. 2039-2054.
27. Sipponen, M.H., et al., *Spatially confined lignin nanospheres for biocatalytic ester synthesis in aqueous media*. Nature Communications, 2018. **9**(1): p. 2300.
28. Tardy, B.L., et al., *Lignin nano- and microparticles as template for nanostructured materials: formation of hollow metal-phenolic capsules*. Green Chemistry, 2018. **20**(6): p. 1335-1344.
29. Figueiredo, P., et al., *In vitro evaluation of biodegradable lignin-based nanoparticles for drug delivery and enhanced antiproliferation effect in cancer cells*. Biomaterials, 2017. **121**: p. 97-108.
30. Han, X., et al., *Green and stable piezoresistive pressure sensor based on lignin-silver hybrid nanoparticles/polyvinyl alcohol hydrogel*. International Journal of Biological Macromolecules, 2021. **176**: p. 78-86.
31. Richter, A.P., et al., *An environmentally benign antimicrobial nanoparticle based on a silver-infused lignin core*. Nature Nanotechnology, 2015. **10**(9): p. 817-823.
32. Figueiredo, P., et al., *Properties and chemical modifications of lignin: Towards lignin-based nanomaterials for biomedical applications*. Progress in Materials Science, 2018. **93**: p. 233-269.
33. Yi, H., et al., *Multilayer composite microcapsules synthesized by Pickering emulsion templates and their application in self-healing coating*. Journal of Materials Chemistry A, 2015. **3**(26): p. 13749-13757.
34. Yang, Y., et al., *Lignin-based Pickering HIPES for macroporous foams and their enhanced adsorption of copper(ii) ions*. Chemical Communications, 2013. **49**(64): p. 7144-7146.
35. Pang, Y., et al., *Lignin-polyurea microcapsules with anti-photolysis and sustained-release performances synthesized via pickering emulsion template*. Reactive and Functional Polymers, 2018. **123**: p. 115-121.
36. Pang, Y., et al., *Preparation and application performance of lignin-polyurea composite microcapsule with controlled release of avermectin*. Colloid and Polymer Science, 2020. **298**(8): p. 1001-1012.
37. Gan, M., et al., *Molecularly imprinted polymers derived from lignin-based Pickering emulsions and their selectively adsorption of lambda-cyhalothrin*. Chemical Engineering Journal, 2014. **257**: p. 317-327.
38. Li, X., et al., *Acetone/Water Cosolvent Approach to Lignin Nanoparticles with Controllable Size and Their Applications for Pickering Emulsions*. ACS Sustainable Chemistry & Engineering, 2021. **9**(15): p. 5470-5480.
39. Frangville, C., et al., *Fabrication of Environmentally Biodegradable Lignin Nanoparticles*. 2012. **13**(18): p. 4235-4243.
40. Li, H., et al., *Self-assembly of kraft lignin into nanospheres in dioxane-water mixtures %J Holzforschung*. 2016. **70**(8): p. 725-731.
41. Li, H., et al., *Preparation of Nanocapsules via the Self-Assembly of Kraft Lignin: A Totally Green Process with Renewable Resources*. ACS Sustainable Chemistry & Engineering, 2016. **4**(4): p. 1946-1953.

42. Beisl, S., A. Friedl, and A. Miltner, *Lignin from Micro- to Nanosize: Applications*. Int J Mol Sci, 2017. **18**(11).
43. Österberg, M., et al., *Spherical lignin particles: a review on their sustainability and applications*. Green Chemistry, 2020. **22**(9): p. 2712-2733.
44. Tang, Q., et al., *Lignin-Based Nanoparticles: A Review on Their Preparations and Applications*. Polymers, 2020. **12**(11): p. 2471.
45. Figueiredo, P., et al., *Green Fabrication Approaches of Lignin Nanoparticles from Different Technical Lignins: A Comparison Study*. ChemSusChem, 2021. **14**(21): p. 4718-4730.
46. Chen, L., et al., *Lignin Nanoparticles: Green Synthesis in a γ -Valerolactone/Water Binary Solvent and Application to Enhance Antimicrobial Activity of Essential Oils*. ACS Sustainable Chemistry & Engineering, 2020. **8**(1): p. 714-722.
47. Sipponen, M.H., et al., *Understanding Lignin Aggregation Processes. A Case Study: Budesonide Entrapment and Stimuli Controlled Release from Lignin Nanoparticles*. ACS Sustainable Chemistry & Engineering, 2018. **6**(7): p. 9342-9351.
48. Tian, D., et al., *Valorizing Recalcitrant Cellulolytic Enzyme Lignin via Lignin Nanoparticles Fabrication in an Integrated Biorefinery*. ACS Sustainable Chemistry & Engineering, 2017. **5**(3): p. 2702-2710.
49. Dai, L., et al., *Lignin-Based Nanoparticles Stabilized Pickering Emulsion for Stability Improvement and Thermal-Controlled Release of trans-Resveratrol*. ACS Sustainable Chemistry & Engineering, 2019. **7**(15): p. 13497-13504.
50. Lievonen, M., et al., *A simple process for lignin nanoparticle preparation*. Green Chemistry, 2016. **18**(5): p. 1416-1422.
51. Lintinen, K., et al., *Antimicrobial Colloidal Silver–Lignin Particles via Ion and Solvent Exchange*. ACS Sustainable Chemistry & Engineering, 2019. **7**(18): p. 15297-15303.
52. Zhao, W., et al., *From lignin association to nano-/micro-particle preparation: extracting higher value of lignin*. Green Chemistry, 2016. **18**(21): p. 5693-5700.
53. Agustin, M.B., et al., *Rapid and Direct Preparation of Lignin Nanoparticles from Alkaline Pulping Liquor by Mild Ultrasonication*. ACS Sustainable Chemistry & Engineering, 2019. **7**(24): p. 19925-19934.
54. Li, Z., et al., *Biomimetic water-in-oil water/pMDI emulsion as an excellent ecofriendly adhesive for bonding wood-based composites*. Journal of Hazardous Materials, 2020. **396**: p. 122722.
55. Moreno, A. and M.H. Sipponen, *Biocatalytic nanoparticles for the stabilization of degassed single electron transfer-living radical pickering emulsion polymerizations*. Nat Commun, 2020. **11**(1): p. 5599.
56. Richter, A.P., et al., *An environmentally benign antimicrobial nanoparticle based on a silver-infused lignin core*. Nat Nanotechnol, 2015. **10**(9): p. 817-23.
57. Klein, S.E., et al., *Unmodified kraft lignin isolated at room temperature from aqueous solution for preparation of highly flexible transparent polyurethane coatings*. RSC Advances, 2018. **8**: p. 40765 - 40777.
58. Klein, S.E., et al., *Unmodified kraft lignin isolated at room temperature from aqueous solution for preparation of highly flexible transparent polyurethane coatings*. RSC Advances, 2018. **8**(71): p. 40765-40777.
59. Witzler, M., et al., *Lignin-Derived Biomaterials for Drug Release and Tissue Engineering*. Molecules, 2018. **23**(8): p. 1885.
60. Alzagameem, A., et al., *Lignocellulosic Biomass as Source for Lignin-Based Environmentally Benign Antioxidants*. Molecules, 2018. **23**(10): p. 2664.
61. Yang, W., et al., *Effect of cellulose and lignin on disintegration, antimicrobial and antioxidant properties of PLA active films*. Int J Biol Macromol, 2016. **89**: p. 360-8.

62. Lobo, F.C.M., et al., *An Overview of the Antimicrobial Properties of Lignocellulosic Materials*. *Molecules*, 2021. **26**(6).
63. McClements, D.J., *Critical review of techniques and methodologies for characterization of emulsion stability*. *Crit Rev Food Sci Nutr*, 2007. **47**(7): p. 611-49.
64. Trujillo-Cayado, L.A., et al., *A Further Step in the Development of Oil-in-Water Emulsions Formulated with a Mixture of Green Solvents*. *Industrial & Engineering Chemistry Research*, 2016. **55**(27): p. 7259-7266.
65. McClements, D.J., *Food Emulsions: Principles, Practices, and Techniques, Third Edition (3rd ed.)*. 2015.
66. Maindarkar, S.N., P.M.M. Bongers, and M.A. Henson, *Predicting the effects of surfactant coverage on drop size distributions of homogenized emulsions*. *Chemical Engineering Science*, 2013. **89**: p. 102-114.
67. Mikkonen, K.S., *Strategies for structuring diverse emulsion systems by using wood lignocellulose-derived stabilizers*. *Green Chemistry*, 2020. **22**(4): p. 1019-1037.
68. Ozturk, B. and D.J. McClements, *Progress in natural emulsifiers for utilization in food emulsions*. *Current Opinion in Food Science*, 2016. **7**: p. 1-6.
69. McClements, D.J., L. Bai, and C. Chung, *Recent Advances in the Utilization of Natural Emulsifiers to Form and Stabilize Emulsions*. *Annu Rev Food Sci Technol*, 2017. **8**: p. 205-236.
70. Carvalho, D.M.d., et al., *Active role of lignin in anchoring wood-based stabilizers to the emulsion interface*. *Green Chemistry*, 2021. **23**(22): p. 9084-9098.
71. Bertolo, M.R.V., et al., *Lignins from sugarcane bagasse: Renewable source of nanoparticles as Pickering emulsions stabilizers for bioactive compounds encapsulation*. *Industrial Crops and Products*, 2019. **140**: p. 111591.
72. Bai, L., et al., *Adsorption and Assembly of Cellulosic and Lignin Colloids at Oil/Water Interfaces*. *Langmuir*, 2019. **35**(3): p. 571-588.
73. Ma, Y., et al., *Synthesis and optimization of polyurethane microcapsules containing [BMIm]PF6 ionic liquid lubricant*. *Journal of Colloid and Interface Science*, 2019. **534**: p. 469-479.
74. Wei, Z., et al., *Alkaline lignin extracted from furfural residues for pH-responsive Pickering emulsions and their recyclable polymerization*. *Green Chemistry*, 2012. **14**(11): p. 3230-3236.
75. Sharma, R., S.M. Jafari, and S. Sharma, *Antimicrobial bio-nanocomposites and their potential applications in food packaging*. *Food Control*, 2020. **112**: p. 107086.
76. Al-Tayyar, N.A., A.M. Youssef, and R. Al-hindi, *Antimicrobial food packaging based on sustainable Bio-based materials for reducing foodborne Pathogens: A review*. *Food Chemistry*, 2020. **310**: p. 125915.
77. Topuz, F. and T. Uyar, *Antioxidant, antibacterial and antifungal electrospun nanofibers for food packaging applications*. *Food Res Int*, 2020. **130**: p. 108927.
78. Gordobil, O., et al., *Potential use of kraft and organosolv lignins as a natural additive for healthcare products*. *RSC Advances*, 2018. **8**(43): p. 24525-24533.
79. Domínguez-Robles, J., et al., *Lignin/poly(butylene succinate) composites with antioxidant and antibacterial properties for potential biomedical applications*. *International Journal of Biological Macromolecules*, 2020. **145**: p. 92-99.
80. Kaur, R., S.K. Uppal, and P. Sharma, *Antioxidant and Antibacterial Activities of Sugarcane Bagasse Lignin and Chemically Modified Lignins*. *Sugar Tech*, 2017. **19**(6): p. 675-680.
81. Alzagameem, A., et al., *Antimicrobial Activity of Lignin and Lignin-Derived Cellulose and Chitosan Composites against Selected Pathogenic and Spoilage Microorganisms*. 2019. **11**(4): p. 670.
82. Qazi, S.S., et al., *Antioxidant Activity of the Lignins Derived from Fluidized-Bed Fast Pyrolysis*. *Molecules*, 2017. **22**(3).

83. Lobo, V., et al., *Free radicals, antioxidants and functional foods: Impact on human health*. Pharmacogn Rev, 2010. **4**(8): p. 118-26.
84. Crouvisier-Urien, K., et al., *Functionalization of chitosan with lignin to produce active materials by waste valorization*. Green Chemistry, 2019. **21**(17): p. 4633-4641.
85. Yang, W., et al., *Valorization of Acid Isolated High Yield Lignin Nanoparticles as Innovative Antioxidant/Antimicrobial Organic Materials*. ACS Sustainable Chemistry & Engineering, 2018. **6**(3): p. 3502-3514.
86. Yang, W., et al., *Enhancing the Radical Scavenging Activity and UV Resistance of Lignin Nanoparticles via Surface Mannich Amination toward a Biobased Antioxidant*. Biomacromolecules, 2021. **22**(6): p. 2693-2701.
87. Sun, S.-N., et al., *Structural Features and Antioxidant Activities of Lignins from Steam-Exploded Bamboo (*Phyllostachys pubescens*)*. Journal of Agricultural and Food Chemistry, 2014. **62**(25): p. 5939-5947.
88. Mahdi Jafari, S., Y. He, and B. Bhandari, *Nano-Emulsion Production by Sonication and Microfluidization—A Comparison*. International Journal of Food Properties, 2006. **9**(3): p. 475-485.
89. Felix, M., A. Guerrero, and C. Carrera-Sánchez, *Optimization of Multiple W1/O/W2 Emulsions Processing for Suitable Stability and Encapsulation Efficiency*. Foods, 2022. **11**(9): p. 1367.
90. Guendez, R., et al., *Determination of low molecular weight polyphenolic constituents in grape (*Vitis vinifera* sp.) seed extracts: Correlation with antiradical activity*. Food Chemistry, 2005. **89**(1): p. 1-9.
91. Guendez, R., et al., *Determination of low molecular weight polyphenolic constituents in grape (*Vitis vinifera* sp.) seed extracts: Correlation with antiradical activity*. Food Chemistry, 2005. **89**: p. 1-9.
92. Czaikoski, A., et al., *Lignin derivatives stabilizing oil-in-water emulsions: Technological aspects, interfacial rheology and cytotoxicity*. Industrial Crops and Products, 2020. **154**: p. 112762.
93. Alzagameem, A., et al., *Lignocellulosic Biomass as Source for Lignin-Based Environmentally Benign Antioxidants*. Molecules : A Journal of Synthetic Chemistry and Natural Product Chemistry, 2018. **23**.
94. Khaldi-Hansen, B.E., M. Schulze, and B. Kamm. *Qualitative and Quantitative Analysis of Lignins from Different Sources and Isolation Methods for an Application as a Biobased Chemical Resource and Polymeric Material*. 2016.
95. Alzagameem, A., et al., *Antimicrobial Activity of Lignin and Lignin-Derived Cellulose and Chitosan Composites Against Selected Pathogenic and Spoilage Microorganisms*. Polymers (Basel), 2019. **11**(4).
96. Wang, G., et al., *Successive ethanol–water fractionation of enzymatic hydrolysis lignin to concentrate its antimicrobial activity*. Journal of Chemical Technology & Biotechnology, 2018. **93**(10): p. 2977-2987.
97. Wang, G., et al., *Subdivision of bamboo kraft lignin by one-step ethanol fractionation to enhance its water-solubility and antibacterial performance*. Int J Biol Macromol, 2019. **133**: p. 156-164.